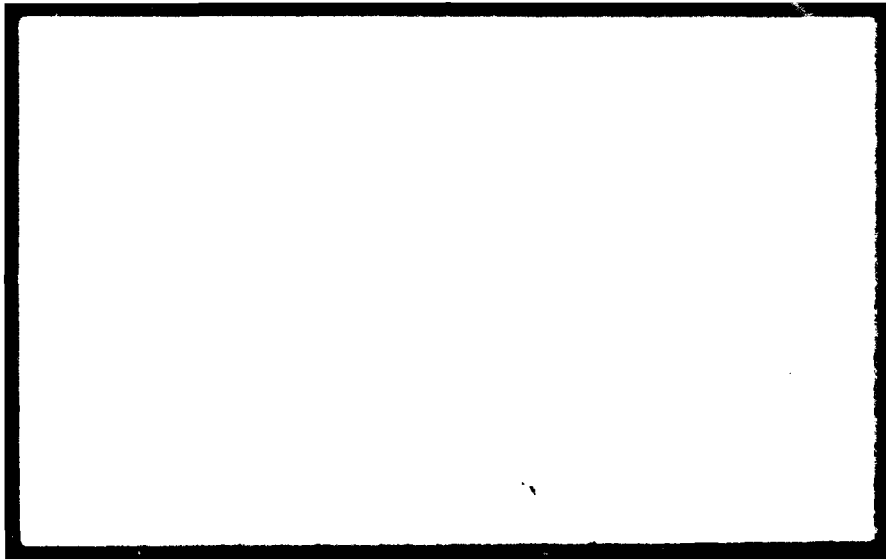


MICROCOPY RESOLUTION TEST CHART
NATIONAL BUREAU OF STANDARDS-1963-A



12

12
PUBLIC
MAY 5 1981
C

THE WEAR OF POLYMERS BY TRANSFER TO
HARD, ROUGH SURFACES

FINAL REPORT

Norman S. Eiss, Jr.

Professor of Mechanical Engineering

27 February 1981

U. S. Army Research Office

Grant No. DAAG 29-77-G-0102

VIRGINIA POLYTECHNIC INSTITUTE AND STATE UNIVERSITY
BLACKSBURG, VIRGINIA 24061

Approved for Public Release; Distribution Unlimited

The findings in this report are not to be construed as an official Department of the Army position unless so designated by other authorized documents.

SECURITY CLASSIFICATION OF THIS PAGE (When Data Entered)

REPORT DOCUMENTATION PAGE		READ INSTRUCTIONS BEFORE COMPLETING FORM
1. REPORT NUMBER <i>(11) 14688, 4-E</i>	2. GOVT ACCESSION NO. <i>AD-A098 478</i>	3. RECIPIENT'S CATALOG NUMBER
4. TITLE (and Subtitle) The Wear of Polymers by Transfer to Hard, Rough Surfaces.	5. TYPE OF REPORT & PERIOD COVERED <i>Final Report</i> 1 Mar 1977-31 Dec 1980	6. PERFORMING ORG. REPORT NUMBER
		8. CONTRACT OR GRANT NUMBER(s) DAAG 29-77-G-0102
7. AUTHOR(s) Norman S. Eiss, Jr.	<i>(12) 110 / 15</i>	10. PROGRAM ELEMENT, PROJECT, TASK AREA & WORK UNIT NUMBERS
9. PERFORMING ORGANIZATION NAME AND ADDRESS Research Division Virginia Polytechnic Institute and State Univ. Blacksburg, Virginia 24061	11. CONTROLLING OFFICE NAME AND ADDRESS U. S. Army Research Office Post Office Box 12211 Research Triangle Park, NC 27709	12. REPORT DATE 27 Feb 1981
14. MONITORING AGENCY NAME & ADDRESS (if different from Controlling Office)	13. NUMBER OF PAGES	15. SECURITY CLASS. (of this report) Unclassified
16. DISTRIBUTION STATEMENT (of this Report) Approved for public release; distribution unlimited.		15a. DECLASSIFICATION/DOWNGRADING SCHEDULE
17. DISTRIBUTION STATEMENT (of the abstract entered in Block 20, if different from Report)		
18. SUPPLEMENTARY NOTES The findings in this report are not to be construed as an official Department of the Army position, unless so designated by other authorized documents.		
19. KEY WORDS (Continue on reverse side if necessary and identify by block number) Polymers, plastics, wear, wear models, low density polyethylene, polyvinyl chloride, polychlorotrifluoroethylene, molecular weight, surface roughness, surface topography, poly(chloro-p-xylene), friction, bearing area ratio, sliding speed		
20. ABSTRACT (Continue on reverse side if necessary and identify by block number) A surface topography characterization system consisting of a Talysurf 4 profilometer, Zonic analog-to-digital converter and Fast Fourier Transform (FFT), and a Tetronix 4051 minicomputer was interfaced to an IBM 370 digital computer. Software for the computation of several surface parameters and for wear models have been written. Single traversal wear experiments were performed on a pin-on-disk machine at sliding velocities less than 1 cm/s. Experiments run at a constant <i>→ next</i> <i>(continued on back)</i>		

Abstract (continued)

bearing area ratio showed no difference in the wear rates of PVC and PCTFE while the wear rates of LDPE were less than both on ground surfaces. The presence of a vapor deposited film of poly (chloro-p-xylylene) did not affect the wear of PVC and PCTFE but reduced the wear of LDPE. A wear model was developed which correctly predicted the decrease in wear rate which occurs as the surface voids fill up with polymer debris, and the maximum wear which occurs as the bearing area ratio is increased. Multiple traversal wear experiments were run at sliding velocities up to 1.4 m/s using LDPE and PVC pins on steel disks. PVC with a molecular weight of 40000 had higher wear rates than 70000 MW PVC except when calculated temperatures exceeded the glass transition temperature. A pin-on-disk wear machine was fabricated with a speed range from 3 to 4400 rpm, a test chamber with temperature controlled up to 300 C, and a low inertia pneumatic loading piston.

PERSONNEL

The following is a list of personnel who were employed on this project, or whose experimental work was supported by this project, and the advanced degrees earned.

- Dr. Norman S. Eiss, Jr., Professor, Mechanical Engineering, VPI&SU,
Principal Investigator
- M. M. Bayraktaroglu, Graduate Research Assistant, Master of Science,
August 1978
- K. A. Smyth, Graduate Research Assistant, Master of Science,
August 1979
- G. S. Vincent, Fellowship Recipient, Master of Science, March 1980
- S. F. McClesky, Graduate Research Assistant, Master of Science,
(non thesis), December 1980
- J. H. Herold, Graduate Research Assistant, Doctor of Philosophy,
June 1980
- C. Mayer, Austrian Exchange Student-Undergraduate Research Assistant,
June-August 1978
- B. Burstrom, Swedish Exchange Student-Undergraduate Research
Assistant, June-August 1979
- B. Jacobsen, Undergraduate Research Assistant, April-June 1980
- M. Dobie, Graduate Research Assistant, September-December 1980

Accession For	
NTIS GRA&I	<input checked="" type="checkbox"/>
DTIC TAB	<input type="checkbox"/>
Unannounced	<input type="checkbox"/>
Justification	
By _____	
Distribution/	
Availability Codes	
_____ or _____	

A

PUBLICATIONS, THESES, AND DISSERTATIONS

Journal Articles, Special Publications

Eiss, N. S., Jr., and Bayraktaroglu, M. M., "The Effect of Surface Roughness on the Wear of Low-Density Polyethylene, ASLE Trans., Vol. 23, No. 3, July 1980, pp. 269-278

Eiss, N. S., Jr., "Characterization of Surfaces in Wear Tests" in Wear Tests for Polymers Selection and Use: Ed. by Bayer, R., ASTM-STP 701, American Society for Testing and Materials, Phila., Pa., 1979, pp. 18-31

Eiss, N. S., Jr., Wood, K. C., Herold, J. H., and Smyth, K. A., "Model for the Transfer of Polymer to Rough, Hard Surfaces," Trans. ASME, Jl. Lub. Tech., Vol. 101, No. 2, April 1979, p. 212

Papers Accepted for Journal Articles, Special Publications

Eiss, N. S., Jr. and Vincent, G. S., "The Effect of Molecular Weight, Surface Roughness, and Sliding Speed on the Wear of Rigid Polyvinyl Chloride." Accepted for presentation at the ASLE Annual Meeting, May 11-14, 1981 and for publication in ASLE Transactions, Reprint No. 81-AM-2D-1.

Eiss, N. S., Jr., and Smyth, K. A., "The Wear of Polymers Sliding on Polymeric Films Deposited on Rough Surfaces," ASME paper No. 80-C2/Lub-24 accepted for publication in Trans. ASME, Jl. Lub. Tech.

Eiss, N. S., Jr., "Wear Testing, Correlation with End-Use Performance," accepted for publication in ASTM-STP, 726. Physical Testing of Plastics.

Eiss, N. S., Jr., "Wear of Non-Metallic Materials" accepted for publication in the Lubrication Handbook, CRC Press.

Master's Theses:

Vincent, G. S., "The Effects of Molecular Weight, Surface Roughness, and Sliding Speed on the Friction and Wear of Polyvinyl Chloride on Steel," March 1980

Smyth, K. A., "A Study of Polymer Wear by Abrasive and Adhesive Mechanisms," August 1979

Bayraktaroglu, M. M., "Influence of Surface Roughness and Sliding Speed on the Friction and Wear of Low Density Polyethylene," August 1978

Dissertation:

Herold, J. H., "A Model for Abrasive Polymer Wear," June 1980.

TABLE OF CONTENTS

	page
ABSTRACT	
PERSONNEL	111
PUBLICATIONS, THESES, AND DISSERTATIONS	iv
LIST OF FIGURES	vi
LIST OF TABLES	vii
INTRODUCTION	1
SURFACE TOPOGRAPHY CHARACTERIZATION	2
SINGLE TRAVERSAL EXPERIMENTS	4
WEAR MODELS FOR SINGLE TRAVERSAL SLIDING	13
MULTIPLE TRAVERSAL SLIDING	17
PIN-ON-DISK WEAR MACHINE	20
CONCLUSION	24
REFERENCES	25
APPENDICES	
A. Single Traversal Wear Data	26
B. A Model for the Abrasive Wear of Polymers	37
C. The Effect of Molecular Weight, Surface Roughness, and Sliding Speed on the Wear of Rigid Polyvinyl Chloride	70

List of Figures

	page
1. Single Traversal Wear of PVC I and PVC II on Disk A	9
2. Single Traversal Wear of PVC I and PVC II on Disk C	10
3. Single Traversal Wear of PVC I and PVC II on Disks MB and ME	12
4. Pin-on-Disk Wear Machine	23
B1 Cross section of a deterministic surface	45
B2 PCTFE wear particles on a deterministic surface	46
B3 LDPE wear deposits on a deterministic surface	48
B4 PTFE wear deposits on a deterministic surface	49
B5 Typical bearing area curves for abrading surfaces	51
B6 Cross section of wear particle and void space	53
B7 Modelled wear as a function of slider length for medium and rough surfaces	58
B8 Wear rate as a function of Bearing Area Ratio	65
C1 Wear of PVC I on steel as a function of number of passes and R_a roughness	78
C2 Wear Rate of PVC as a function of molecular weight, R_a roughness, and sliding speed	80
C3 Coefficient of friction for PVC I sliding on steel as a function of number of passes, sliding speed, and R_a roughness	81
C4 Wear rate plotted on log-log scales to show R_a roughness dependence	86
C5 Steel surface with deposits of PVC I, 60 passes, 0.10 m/s	90
C6 Steel surface with deposits of PVC I, 400 passes, 0.10 m/s	90
C7 Steel surface with deposits of PVC II, 400 passes, 0.10 m/s	92
C8 Steel Surface with deposits of PVC II, 1600 passes, 0.10 m/s	92
C9 Tensile force versus cross head motion in elevated temperature tests of PVC I	93

List of Tables

	page
A1 Single Traversal Wear Results, Experiment 1, (LDPE, PVC, and PCTFE, Radial Lay Disks)	28
A2 Single Traversal Wear Results, Experiment 2, (LDPE, PVC, and PCTFE, Unidirectional Lay Disks, Polymer Coating)	30
A3 Single Traversal Wear Results, Experiment 3, (PVC I and II, Unidirectional Lay Disks)	33
B1 Wear Rates and G Factors	61
C1 Polymer Mechanical Properties	74
C2 Surface Parameters for Steel Disks	76
C3 Calculated Surface Temperatures, PVC Sliding on Steel at 1.4 m/s	82
C4 Number of Contacting Peaks and Average Penetration Depth	88

INTRODUCTION

In recognition of the increasing use of polymers for applications in which their tribological properties were important, the U. S. Army Research Office funded a three-year research program* at VPI&SU to study the wear of polymers by transferred films. During this program a wear measuring technique was developed using Neutron Activation Analysis (NAA) [1]**. The technique was capable of detecting less than one microgram of polymer transferred to a steel counterface. Using this technique, the wear of PCTFE sliding on a ground steel surface was measured as a function of the surface roughness [2] and the direction of the lay relative to the sliding direction [3]. A wear model was developed in which the polymer properties and the surface topography of the steel were used to predict the relative wear of PVC and PCTFE which agreed with the wear measurements [4]. At the conclusion of this research it was recognized that the roughness of the steel surface was one of the most significant factors influencing the wear of polymers, and that models incorporating surface roughness parameters were capable of predicting the relative wear of polymers [5].

A continuation of this research was funded by the U. S. Army Research Office for the period of 1 March 1977 to 31 December 1980***.

* GRANT DA-ARO-D-31-124-73-G170, 1 September 1973-31 August 1974
GRANT DAHCO 4-75-G-0008, 1 September 1974-31 August 1975
GRANT DAAG 29-76-G-0009, 1 September 1975-30 November 1976

** Numbers in brackets refer to references listed in the Reference section

*** GRANT DAAG 29-77-G-0102

The summary of this research is the subject of this final report. During this research a surface topography measurement system was interfaced with a digital computer and software was developed for the characterization of surface topography. Wear models were developed to predict the wear of polymers in single traversal experiments. Wear measurements were compared with the predictions and found to agree within an order of magnitude of each other. Experiments were run to measure the wear of polymers making multiple passes over rough steel surfaces at sliding speeds where interfacial heating was significant. A new pin-on-disk wear machine with a greater sliding speed range and a heated test chamber was designed and built in the latter stages of the research. Summaries of these research activities are given in the following sections.

SURFACE TOPOGRAPHY CHARACTERIZATION

By 1975, we had made sufficient observations of the transfer of polymers to rough surfaces to realize that a complete characterization of the topographical features of the rough surface was necessary if transfer and wear models were to be developed. During this period surface topography characterization was subcontracted to laboratories which had the necessary measurement systems. This procedure was unsatisfactory because of the time required to transport specimens to and from the laboratories. It was also impossible to quickly monitor the roughness of surfaces as they were machined in our shops. Therefore, we acquired a surface profilometer system prior to the start of the research summarized in this report.

The system consisted of a Talysurf 4 profilometer, a Zonic analog-to-digital converter and fast-fourier transform (FFT) analyzer and a

6

Tetronix 4051 microcomputer. Initially digitized profile data was analyzed using programs executed by the 4051. However, the computation time was slow compared to the IBM 370 computer. Therefore, the interface between the Zonic FFT and the IBM 370 was made and all profile data was transmitted to the IBM 370. Software was written for the calculation of surface parameters. In addition, several special programs and the wear model programs were prepared using the interactive, timesharing mode of the IBM 370.

The surface parameters which are routinely calculated include R_a (arithmetic average), RMS, skewness, kurtosis, R_t (maximum peak-to-valley), average slope, mean peak curvature, BAC (bearing area curve, ADF (amplitude density function), ACF (autocorrelation function), and PSD (power spectral density). In addition, programs have been written to calculate these parameters for only those portions of the profile above a specified height level.

One of the special programs was written to recreate the actual surface from the profile by considering the shape of the stylus. The stylus tip is a pyramid with a 90 degree included angle and a tip radius of 2.5 μm . Thus, as the stylus moves over a peak on the surface the radius of the profile peak is equal to the radius of the surface peak plus the radius of the stylus tip [6]. This program uses this relationship to obtain the actual surface topography from the profile generated by the stylus motion.

SINGLE TRAVERSAL EXPERIMENTS

The wear experiments performed on the previous grants indicated that the polymer transferred to the rough metal surfaces at discrete sites such as high asperities on ground or bead blasted surfaces or in abrasive scratches on polished surfaces [1]. It was also noted that in multiple traversal experiments the polymer wear debris collected in the low points on the surface and eventually filled in the surface to the point where the normal load was supported by the debris. This process was accompanied by a decrease in wear rate [2]. It was decided to perform single traversal wear experiments so that the interaction between the polymer and the asperities of the rough surface could be studied without the influence of accumulating wear debris.

Single traversal wear experiments were used to observe the discrete nature of the wear process and to provide wear measurements to compare to values predicted by the wear models. The scanning electron microscope (SEM) was the major tool used to observe the polymer and the surface after wear had occurred. These observations were used primarily as input to the wear models described in the next section. In this section the wear experiments will be described and the results will be discussed.

Three major single-traversal experiments were performed. In the first experiment, PVC, PCTFE, and LDPE pins were worn on rotating steel disks which were ground with a radial lay. The radial lay was chosen because the sliding direction would always be perpendicular to the lay as the disk rotated. It was believed that this relationship between the

lay and the sliding direction would be easiest to model because surface profiles taken perpendicular to the lay would be representative of the surface that the polymer pin encountered. The experimental conditions and the wear results for Experiment 1 are described in Appendix A, Table A1 and Ref. 4 and 7.

In the second experiment, PVC, PCTFE, and LDPE pins were worn on rotating steel disks which were ground with a unidirectional lay. In these experiments it was desired to have several disks ground to surface roughnesses which were as alike as possible. By grinding several disks at once on a surface grinder uniformity was obtained. The disks with the radial lay in Experiment 1 were ground one at a time on a cutter and tool grinder so that uniformity was difficult to achieve. When the sliding direction was parallel to the lay direction the wear rate decreased sharply; thus the wear rate was not uniform over the circular wear path. In Experiment 2 the normal load and apparent area of contact were chosen so that all polymers had a ratio of calculated real area to apparent area, BAR, of 0.11. A constant BAR was chosen so that the wear of each polymer was a result of encountering the uppermost parts of the surface to the same extent. In half of the experiments, the steel disks was vapor deposited with a 50 μm thick coating of poly (chloro-p-xylylene) prior to the wear test. The experimental conditions and the wear results for experiment 2 are described in Appendix A, Table A2 and in Ref. 8.

In the third experiment, PVC pins with molecular weights of 40,000 and 70,000 were worn on rotating steel disks which were ground with a unidirectional lay. In these experiments the BAR's were varied by changing the normal load and the apparent area of contact. Since there

was no difference in the yield strengths of the PVC with the different molecular weights the same loads and apparent areas for each resulted in the same BAR. Therefore, the wear rates of the polymers as a function of molecular weight were compared at the same load and BAR. The description of the experimental conditions and the wear results are given in Appendix A, Table A3.

One purpose for collecting the data from these three experiments in this report is to be able to compare results from the different experiments and to examine the variability of the measured wear rates. Some of the data in these experiments are presented and discussed in the following paragraphs.

In Experiment 1 the highest wear rates were recorded on disk 19. The surface roughness parameters indicated that disk 19 had the largest positive skewness, and the largest peak-to-valley height of any of the disks. The penetration of the steel asperities into the polymer was also calculated to be higher than any of the other polymer-disk combinations. Hence, the high rates of wear on disk 19 were consistent with its surface roughness.

However, the data do not show a consistent relationship between the relative wear rates of PVC and PCTFE. Evidence of this inconsistency is given by the following examples. The data obtained on disks 19 and 31 permitted a direct comparison of the wear of PVC and PCTFE on the same portion of each disk. On disk 19, for the same normal load and apparent area of contact PVC had twice the wear rate of PCTFE. On disk 31, PVC had twice the normal load as applied to PCTFE for the same apparent

areas, and its wear rate was only 50 per cent greater than that recorded for PCTFE. PCTFE was also run on disk 31 at the same normal load and apparent area as PVC and the wear of PVC was only 20 per cent larger than that of PCTFE. Disk 33 produced a reversal in the wear of PVC and PCTFE. With the same load and apparent area the PVC wear rate was 30 per cent less than that of PCTFE. These apparently inconsistent results were originally explained in terms of the maximum penetration of the steel asperities into the polymer [4]. However, this explanation was not confirmed in Experiment 2. The data in Experiment 2 for PVC and PCTFE at the same depths of penetration showed no difference in the wear rates of these two materials. In Experiment 2 the same penetration depths were achieved by having the apparent area of PVC equal to 0.22 that of PCTFE for the same normal load.

The above observations prompt a basic question: What conditions should be chosen to measure the relative wear of polymers against hard rough surfaces? If one considers the use of a polymer in a specific application, an appropriate response to this question would be that the apparent pressure must be the same (normal load divided by the apparent area of contact). Testing under constant apparent pressure would be consistent with the intended use of the polymers, vis. the load and apparent area would be dictated by the design requirements and the chosen geometry for the component.

However, if the relative response (wear) of polymers to surface roughness is desired, then it is important that the different polymers experience the same roughness features. In this case, an appropriate

response to the above question would be that the bearing area ratio must be the same, thereby, assuring that sufficient pressure has been applied to each polymer to cause it to be penetrated by the surface features to the same depth. It was this latter response to the question which resulted in choosing a constant bearing area ratio of 0.11 for Experiment 2.

In Experiment 3, several wear measurements were made on one disk with the same polymer pin. Because of the conical shape of the pin, the apparent area increased during each measurement and the bearing area ratio tabulated in Table A3 is the average for each test. The wear rate data has been plotted as a function of BAR for disk A in Fig. 1. For a load of 19.6N it is noted that the wear rate increased for increasing BAR. Where data existed for both molecular weights of PVC at the same BAR, the lower molecular weight PVC had a higher wear rate. For these data at the same normal load the BAR was increased by decreasing the apparent area of the pin. Fig. 1 also shows that reducing the load and the apparent area to obtain the same BAR's as at the higher load, resulted in lower wear rates for the lower normal loads.

The wear rate data in Fig. 2 for disk C extend out to larger BAR's than the data plotted in Fig. 1. The surface characterization parameters for disk A and C are similar and the magnitudes of the wear rates on disk C were in agreement with those measured on disk A. However, the increase in wear rate with BAR appeared to reach a peak between a BAR of 0.3 and 0.4. The scatter in the data is so large that it cannot be determined whether the wear rate stayed constant or decreased after the peak. This observation will be noted again when the wear models are

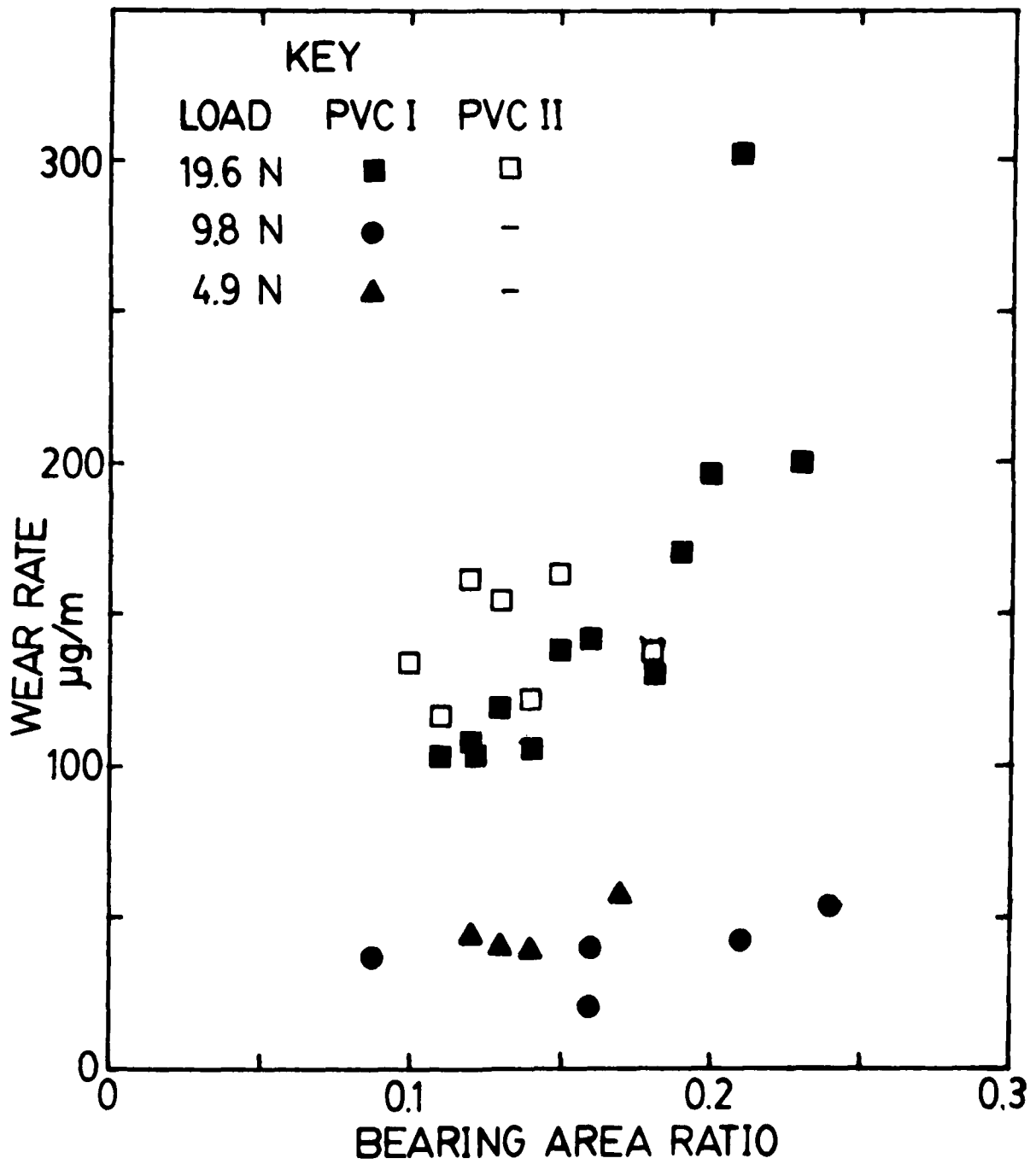


Figure 1. Single traversal wear of PVC I and PVC II on Disk A

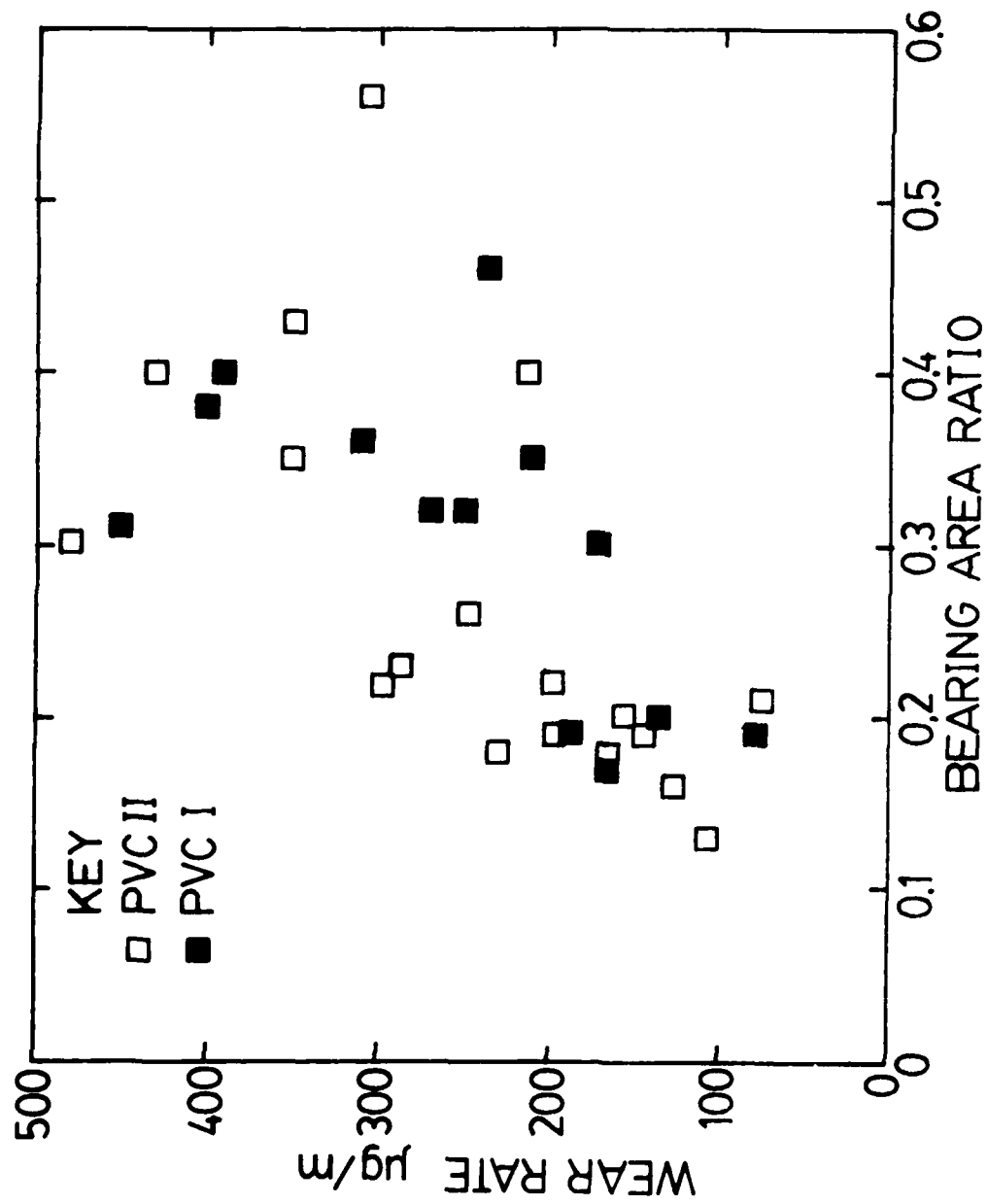


Figure 2. Single traversal wear of PVC I and PVC II on Disk C,
 Normal Load 19.6 N

discussed in the next section and Appendix B. The scatter in the data makes it impossible to state that there is any significant difference in the wear rates caused by the different molecular weights.

The wear rates for both molecular weights and disks MB and ME are shown in Fig. 3. The increase in wear rate with increasing BAR is the same trend as observed on the rougher disk A and C. Again, the scatter in the data makes it impossible to measure a difference between the two molecular weights. A comparison of the data on the disks MB and ME with the data on disk A and C show that wear rates on the rough disks are almost an order of magnitude larger than those on the smoother MB and ME disks at comparable loads and BAR's.

After examining the single-traversal wear data, one cannot help but notice the random nature of the wear rate data. Even repeated tests on the same surfaces with the same experimental conditions did not result in consistent wear rate results. This randomness of the wear process was a function of the randomness of the ground surface. Unfortunately, the sampling of this surface topography by a stylus profilometer resulted in a mechanical filtering of the topography information by the stylus geometry. It is believed that the surface features not detected by the stylus are the major contributions to the randomness of the measured single traversal wear data.

On the other hand, the roughness that was measured by the profilometer was found to correlate quite strongly with the observed wear. The comparison of the wear rates in Figs. 2 and 3 for rough and smooth surfaces illustrate this correlation quite well. The implications of these two observations on the modeling of wear will be discussed in the next section.

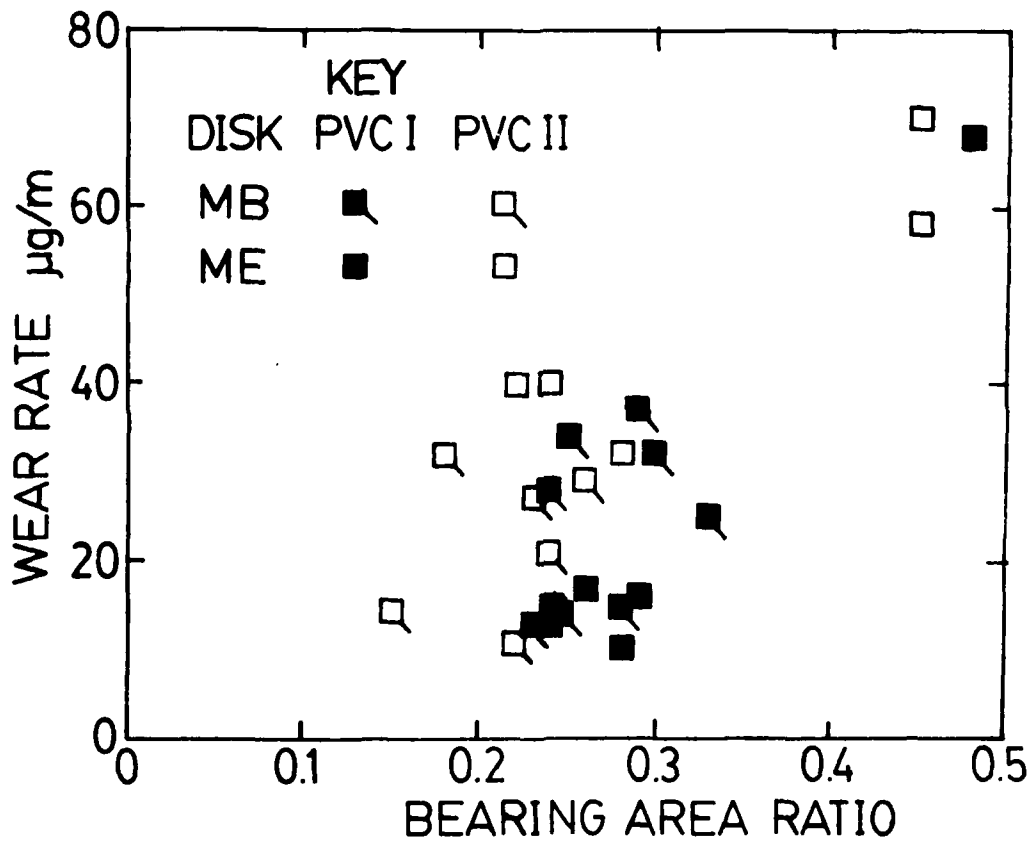


Figure 3. Single traversal wear of PVC I and PVC II on Disks MB and ME, Normal Load 19.6 N

WEAR MODELS FOR SINGLE TRAVERSAL SLIDING

One of the objectives of the research on polymer wear on rough surfaces was to characterize surface roughness with several parameters and then determine which parameters best correlated with the wear measurements. For example, the wear rate of PCTFE was found to correlate with the R_a and the average slope of the rough surface [2]. However, it was soon realized that the interaction between the polymer properties and the surface topography was important in the wear process. Therefore, the wear rates of PCTFE and PVC were related to the depth of penetration of the surface asperities into the polymers [4]. At the same depths of penetration the wear rate of PVC was higher than that of PCTFE. This wear rate difference correlated with the inverse of the energy-to-rupture for these polymers.

The next step in the modeling of single traversal wear was based on the observed deposit angles ϕ of polymer transferred to a rough surface, which were significantly different for PVC, PCTFE, and Nylon 6-6 [4]. The wear at each individual penetrating asperity was modeled as a wedge of polymer. The cross sectional area of the wedge was a right triangle, with a height p_1 equal to the depth of penetration of the asperity into the polymer and the base equal to $p_1/\tan \phi$. For single traversal sliding one wedge of material was assumed to be produced at each asperity. This model was used to calculate wear rates on surfaces on which the polymers had been worn (Appendix A, Table A1). A comparison of the calculated and measured wear rates showed that the predicted wear rates were in agreement with the measured wear for PCTFE, an order of magnitude less than measured wear for PVC, and ranged from a low of a fifth

of the measured wear to a high of 20 times measured wear for LDPE.

Detailed explanations of these results are given in Ref. 8.

This wear model represented a major change from the objective of correlating wear rates with surface parameters or polymer properties. In this model, we attempted to predict the wear rate given certain polymer properties such as yield strength and the deposit angle, the profiles of the rough surface in digital form, and the normal load. The fact that the predicted wear rates were in good agreement with the measured wear rates for at least one of the polymers tested encouraged us to consider refining this model to correct some of its deficiencies and to include some additional features. This refined model is included as Appendix B in this report.

Some of the significant features of this new model were as follows. Only those penetrating asperities which had a slope within the depth of penetration greater than the deposit angle ϕ were assumed to produce a wedge shaped wear particle. This criterion for wear particle formation accounted for the possibility of polymer deforming and passing around a penetrating asperity without removing a wear particle. The number of wedge shaped wear particles which could be produced at a penetrating asperity was limited either by the sliding length of the polymer which the asperity encountered or by the volume of the space between the polymer and metal surface adjacent to the penetrating asperity. The sliding motion was assumed to force the particle in the valley adjacent to the asperity and the particles would continue to accumulate until either the polymer ceased to contact the asperity or until the space was filled

with particles. In the model, the wear from an asperity ceased when there was no more space for wear particles to accumulate,

By including the debris transport in the model, the model was now equally applicable to single- and multi-traversal sliding. For the latter, it was only necessary to multiply the length of the slider measured in the sliding direction by the number of traversals.

A final feature of the model was based on the correlation of polymer wear in single traversal tests with the elongation-to-break for the polymer. The rate of production of wear particles at a penetrating asperity was assumed to be proportional to the elongation-to-break for the polymer. However, the proportionality constant could only be determined experimentally and the constant was found to be significantly different for PVC and PCTFE. Thus, it was concluded that the properties of the polymer, the surface roughness, and the load were not correctly related in the model.

Given several profiles from a surface, the model predicted the variability in wear rates observed in wear experiments. In addition, the model correctly predicted the change in wear rate that occurred as a function of bearing area ratio as shown in Fig. B-8.

A successful wear model must be able to predict quite different mechanisms of transfer. For example, in Appendix B and in Ref. 7 the different mechanisms of transfer of LDPE and the more brittle polymers PCTFE and PVC was noted. LDPE transferred at the points of contact and tended to adhere or mechanically interlock with the asperity. The result was that little subsequent wear occurred at that site. The wear particles for the other two polymers were easily pushed down from the

peak by the oncoming material and a succession of wear particles were produced, which was the process modeled by the wear model. Any further development of wear models must include some method of predicting this difference in the movement of the debris from the point of formation into void spaces.

Debris transport becomes a significant factor in determining the wear rates in multiple traversal experiments. If debris is permitted to accumulate in the valleys between peaks it will eventually support some of the normal load and modify the wear rate. If the debris is removed from the valleys by centrifugal forces, flowing gases or liquids, or by the frictional force between the sliding polymer and the debris, the wear rate may be constant over long running times. In the next section initial multiple-pass sliding experiments are described.

MULTIPLE TRAVERSAL SLIDING

While single-traversal sliding represents one of the least complex systems to study and model, the more common sliding system involves multiple traversal sliding. In multiple traversal sliding the transport of the debris out of the wear track can have a significant influence on the steady state wear rate of the system. Since wear debris transport was not significant in single traversal sliding, and hence could not be studied in these systems, two multiple traversal experiments were performed. One experiment involved the sliding of low density polyethylene (LDPE) on surfaces with R_a values from 0.06 to 1.16 μm at two sliding velocities, 0.32 and 1.28 m/s. [9] The second experiment involved the sliding of two different number molecular weights of PVC, 70000 called PVC I and 40000 called PVC II, on surfaces with R_a values from 0.15 to 1.27 μm at sliding velocities from 0.1 to 1.4 m/s. The manuscript describing this research is included in this report as Appendix C.

The conclusion of both studies was that the wear rates increased with increased surface roughness and with increased sliding speed. The wear mechanism on the rough surfaces was similar for both polymers. The high ridges on the steel surfaces were the sites of wear debris generation although it was not clear whether the wear particles were removed by a cutting action on each pass of the polymer or whether wear particles resulted after multiple encounters with asperities or both. Debris particles accumulated in the valleys near the high ridges and occasionally large mass of wear debris collected on the ridges. Debris particles were moved from the wear track to the surface of the steel disk outside the wear track. The particle sizes were much larger than the spaces

between the highest asperities on the surface indicating that smaller particles agglomerated to form these larger particles. This agglomeration was more prevalent from LDPE than PVC. SEM photos of these observations appear in [9] and Appendix C.

On smooth surfaces the wear mechanism consisted of an initial transfer of polymer to a site on the surface and the growth of these deposits on subsequent passes of the polymer over these sites. However, LDPE deposits often grew into continuous films on the surface while the PVC deposits grew in isolated sites but were removed before they could grow into continuous films. The LDPE films were observed to break up thus exposing the metal surface for continued transfer. Thus, on smooth surfaces an initial transfer was followed by growth due to continued transfer, and the subsequent detachment of a wear particle. In contrast, on the rough surfaces transfer and growth seemed to play a small role in the wear process.

The influence of sliding velocity was primarily through the generation of heating at the interface and the resulting temperature rise. Temperatures were calculated using the Archard flash temperature model (See Appendix C1 for temperatures calculated for PVC). The calculated temperatures were well below the melting temperatures of both LDPE and PVC. While the calculated temperatures were always above the glass transition temperature T_g for LDPE (-120C), they were always below the T_g for PVC (74C) except at the highest sliding speed on the roughest surface. It was found that the wear rate of PVC I was significantly less than that for PVC II unless the calculated temperature was greater than its T_g . In this case there was no significant difference in the

wear rates of PVC I and II. When the temperature exceeded T_g the molecular chains became much more mobile and the generation of wear particles became a function of interchain slip resistance rather than intrachain scission.

It was noted that the wear of PVC I was significantly less than that for PVC II in the multiple pass experiments. However, in the single traversal experiments the scatter in the results was large enough that no significant difference could be observed as a function of molecular weight. One explanation for the larger variability in the single traversal experiments is that the number of individual events which are integrated in the total sliding distance is small compared to the number of events in the multiple pass experiment. The measured wear rate is an estimate of the true wear rate for the system. The measure is more reliable as the number of events which are included in the integration is increased. Thus, the multiple traversal experiments provided a more reliable statistical sampling of the wear events, and permitted the detection of the influence of molecular weight on wear.

PIN-ON-DISK WEAR MACHINE

During this research project two types of wear experiments were run. One type was the single traversal experiment in which the sliding velocity was less than 1 cm/s. The other type was the multiple traversal experiment in which the sliding velocities ranged between 0.1 and 1.4 m/s. One pin-on-disk wear machine was used for both these types of experiments. This wear machine was capable of a continuous speed variation over a range of 30 to 400 RPM. A 100:1 geared speed reducer provided a second range of 0.3 to 4 RPM. The former range was used for the high speed experiments and the latter range for the low speed experiments. The change over from the high range to the low range required that a shaft be replaced with the gear box, a procedure which required repositioning of various components in the drive system. In addition, the existence of only one machine meant that only one experimenter could be doing wear tests at a given time. To provide the opportunity for running low and high speed experiments simultaneously, it was decided to design and build a second pin-on-disk machine.

The new machine has several features not available on the old machine. The drive system utilizes a variable speed transmission which is connected to the disk drive shaft by timing belts and pulleys. Three pulley combinations provide speed ratios of 11:1, 1:1, and 1:11 which in combination with the variable speed transmission provide a maximum rotational speed of the disk of 4400 RPM and a minimum speed of 3 RPM. Thus, the new machine can achieve sliding speeds as high as 10 m/s at a radius of 2.2 cm.

In the old machine, the normal load was applied by dead weight loading by placing mass on a platform located directly over the pin. At high rotational speeds, the runout of the disk caused the mass to accelerate and decelerate vertically, thus creating a variation in the force between the pin and the disk. For example, assume that the load between the pin and the disk is given by $MA\omega^2 \sin\omega t + Mg$ where M is the mass used for the dead weight load, A is the amplitude of the runout of the disk and ω is the circular frequency of rotation. For a rotational speed of 2000 rpm and an amplitude of 0.001 cm the ratio of the term $A\omega^2$ to g is 0.04. However, at 4000 rpm the ratio is 0.18, i.e., there is almost a 20 per cent variation in the normal load caused by the runout. Because one of the primary uses of the new machine was to be high speed testing, one of the criterion for its design was the minimization of the normal load variation due to runout.

One method of controlling runout is to improve the accuracy of machining the disks and decreasing the runout of the platform on which the disk is placed. While both of these methods were used, it also decided to use a pneumatic loading system to reduce the inertial mass attached to the pin. The total inertial mass was reduced to 32 gm. At 4000 rpm and an amplitude of 0.001 cm. the variation in force is 0.056N, thus, if the applied load is 4.9N (equivalent to a dead weight mass of 0.5kg), the load variation is one per cent due to this runout.

The friction force was measured on the old machine by the strain in a cantilever spring which resisted the friction force. In the new machine, the loading assembly for the pin is fastened to a cantilever

beam. The deflection of the cantilever beam by the friction force is measured by a proximity sensor. A proximity sensor is also used to measure the change in length of a pin during a wear experiment. This measurement permits the monitoring of the wear continuously during an experiment and would provide a measure of volumetric loss which could complement a weight loss measurement.

The new machine also has a chamber which surrounds the disk and pin which can be heated to 300 C. The temperature is controlled by a thermocouple in the chamber and an electronic controller. A cut-away view of the machine is shown in Fig. 4.

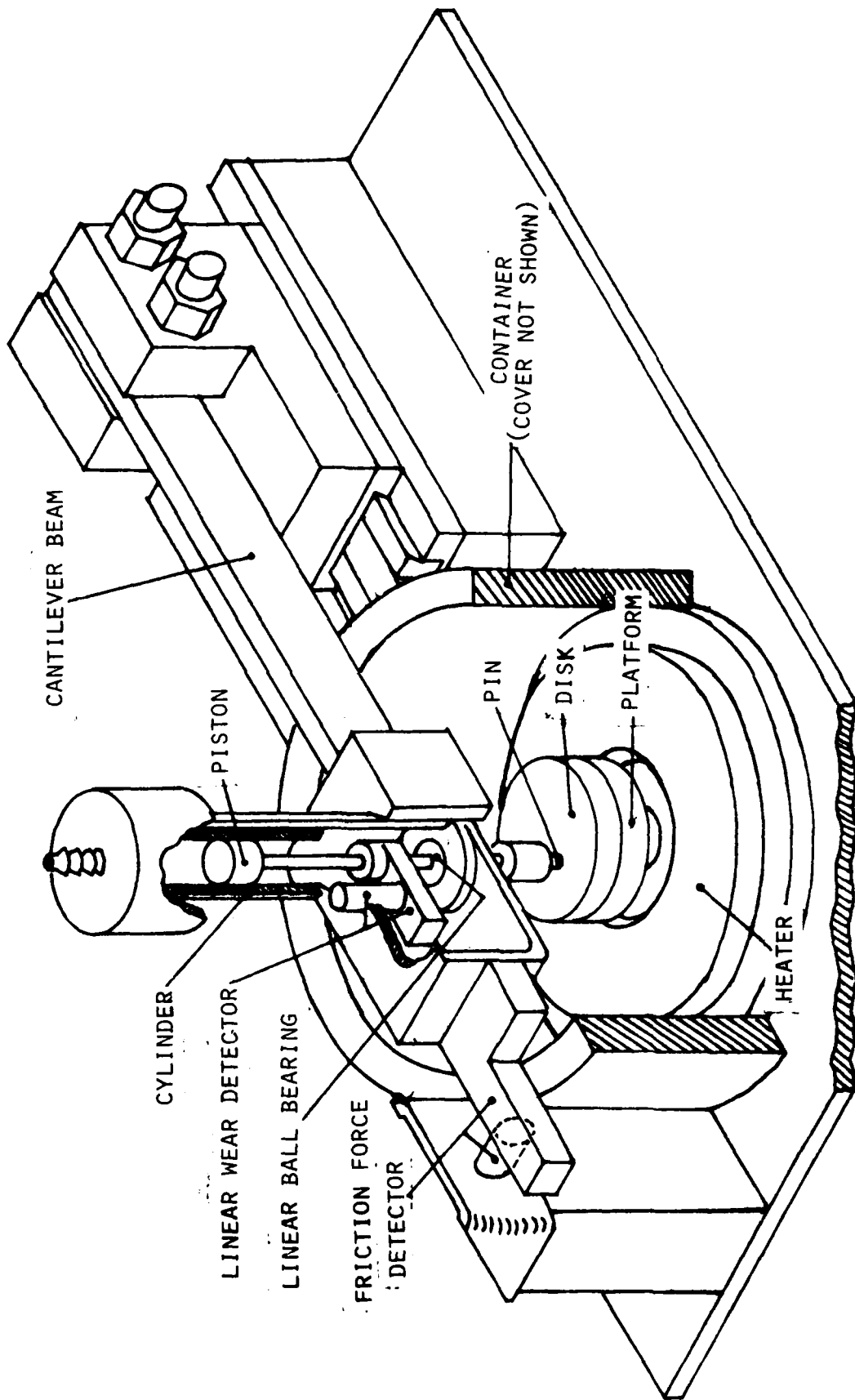


Figure 4. Pin-on-disk wear machine

CONCLUSIONS

The conclusions from the research have been stated in each of the previous sections, in the manuscript in the Appendices, and in the published papers listed in the Reference section. In this section conclusions based on the overview of the research program will be stated. While progress has been made in the understanding of the interaction of the polymer with rough surface through experiments and wear models, the goal of being able to predict wear rates from standardized properties of polymers and detailed characterization of rough surfaces is as elusive as ever. The modeling of single traversal wear for certain types of polymers is still dependent on one or more constants which are determined from wear tests. In addition the single traversal wear tests have an inherent randomness which cannot be modeled. A major limitation is caused by the mechanical filtering of the surface by the profilometer stylus geometry.

No models have been formulated for multiple traversal sliding as yet, but it is clear that such models must incorporate mechanisms of debris transport within and to the outside of the wear track. The interaction between the asperities of the rough surface and the polymer are still the fundamental event to be modeled. However, in multiple traversal sliding a model which requires multiple encounters with an asperity before a particle is produced may be more realistic than the single encounter wear particle model used in the single traversal wear models developed in this research. Thus, future research will concentrate on the multiple traversal sliding and the modeling of this system.*

* ARO Contract DAAG 29-80-C-0115, 14 April 1980 - 13 April 1983

REFERENCES

1. Eiss, N. S., Jr., S. D. Doolittle, and J. H. Warren, "An Application of Neutron Activation Analysis to the Measurement of the Wear of Polymers," Wear, Vol. 38, 1976, pp. 125-139.
2. Eiss, N. S., Jr., and J. H. Warren, "The Effect of Surface Finish on the Friction and Wear of PCTFE Plastic on Mild Steel," Society of Manufacturing Engineers, Paper No. IQ75-125, April 1975.
3. Eiss, N. S., Jr., J. H. Warren, and T. F. J. Quinn, "On the Influence of the Degree of Crystallinity of PCTFE on its Transfer to Steel Surfaces of Different Roughnesses," The Wear of Non-Metallic Materials, Edited by Dowson, D., Godet, M., and Taylor, C. M., Mechanical Engineering Publications, Ltd., London, 1976, pp. 18-24.
4. Warren, J. H., and N. S. Eiss, Jr., "Depth of Penetration as a Predictor of the Wear of Polymers on Hard, Rough Surfaces," Trans. ASME, Journal of Lubrication Technology, Vol. 100, No. 1, Jan. 1978, pp. 92-97.
5. Eiss, N. S. Jr., "The Wear of Polymers by Transferred Films," Final Report submitted to the U.S. Army Research Office, 15 January 1977, 103 pages.
6. Eiss, N. S., Jr., "Characterization of Surfaces in Wear Tests," in Selection and Use of Wear Tests for Polymers, ed. Bayer, R., ASTM-STP 701, American Society for Testing and Materials, Phila., Pa., 1979, pp. 18-31.
7. Eiss, N. S., Jr., and K. A. Smyth "The Wear of Polymers Sliding on Polymeric Films Deposited on Rough Surfaces," ASME Paper No. 80-C2/Lub-24, accepted for publication in the Journal of Lubrication Technology.
8. Eiss, N. S., Jr., K. C. Wood, J. H. Herold, and K. A. Smyth, "Model for the Transfer of Polymer to Rough, Hard Surfaces," Trans. ASME, Journal of Lubrication Technology, Vol. 101, No. 2, April 1979, pp. 212-219.
9. Eiss, N. S., Jr., and M. M. Bayraktaroglu, "The Effect of Surface Roughness on the Wear of Low-Density Polyethylene," ASLE Trans., Vol. 23, No. 3, July 1979, pp. 269-278.

APPENDIX A

Single Traversal Wear Data

TEST CONDITIONS, EXPERIMENT 1

Disks were 1018 steel, ground with a radial lay. Surface topography parameters are the averages of four profiles taken perpendicular to the lay direction.

Experiments were performed on a pin-on-disk apparatus. The polymer pins were truncated cones and the diameters of the apparent areas of contact are tabulated as A_a dia. Polymer properties are summarized in the following table:

	<u>PCTFE</u>	<u>PVC</u>	<u>LDPE</u>
Yield Strength (MPa) (0.2% offset)	23.1	103.	5.70
Elongation to Break (m/m)	1.25	0.26	1.03
Energy to Rupture (MPa m/m)	41.8	24.8	9.6

The bearing area ratios were calculated from $BAR = W/3YA_a$ where W = normal load, Y = yield strength.

The experiments were single-traversal wear paths formed by moving the pin radially each revolution of the disk. The average sliding speed was 0.94 cm/s. The polymer transferred to the disk was measured using Neutron Activation Analysis.

Experiments on disks 1, 2, 3 and 5 were run at a different time and by a different student than those run on other remaining disks.

TABLE A1 SINGLE TRAVERSAL WEAR RESULTS, EXPERIMENT 1

Disk	R _a μm	RMS μm	SKEW	KURT	R _t μm	Polymer	A _a dia. μm	Load N	BAR	Max. Depth μm	Wear Rate μg/m
1	0.21	0.26	-0.72	3.65	1.57	LDPE	991	0.49	0.037	0.22	2.02
						LDPE	462	1.96	0.686	0.70	2.40
						PCTFE	378	4.41	0.569	0.58	2.46
2	0.18	0.25	-1.59	7.71	1.90	LDPE	1223	0.49	0.024	0.11	2.23
						LDPE	429	1.47	0.596	0.46	1.16
						PCTFE	335	2.94	0.602	0.46	1.38
3	0.15	0.22	-2.28	10.26	1.68	LDPE	1124	0.49	0.029	0.09	2.44
						LDPE	458	2.45	0.869	0.51	1.30
5	0.50	0.60	-0.34	2.64	2.81	LDPE	1070	0.49	0.032	0.09	1.15
						LDPE	564	0.98	0.230	0.59	0.33
						PCTFE	437	1.96	0.188	0.53	0.06
19	0.39	0.57	0.41	6.07	4.67	PCTFE	564	0.98	0.057	1.74	2.91*
						PVC	564	0.98	0.013	0.82	5.73*
20	0.39	0.50	-0.50	2.77	2.72	PCTFE	564	0.98	0.057	0.55	0.46
						PVC	564	0.98	0.013	0.31	0.96
31	0.25	0.31	-0.15	2.97	2.07	PCTFE	564	1.96	0.113	0.57	0.89*
						PCTFE	564	0.98	0.057	0.48	0.70*
						PVC	564	1.96	0.025	0.36	1.08*
33	0.42	0.54	-0.41	2.93	2.94	PCTFE	564	1.96	0.113	0.76	2.14
						PVC	564	1.96	0.025	0.42	1.47

* Starred values were obtained by running PVC first, cleaning off the transferred polymer, then running PCTFE at the same radius.

TEST CONDITIONS, EXPERIMENT 2

Disks were 1018 steel, ground with unidirectional lay. Surface topography parameters are the averages of four profiles taken perpendicular to the lay direction.

Experiments were performed on a pin-on-disk apparatus. The polymer pins were truncated cones and the diameters of the apparent areas of contact are tabulated as A_a dia. Polymer properties are the same as those in Experiment 1. The loads, apparent areas, and polymers were selected so that the bearing area ratios for all tests were 0.11.

Other experimental conditions are the same as in Experiment 1.

On the disks XX2, a coating of poly (chloro-p-xylylene) approximately 50 nm thick was applied by vapor deposition prior to running the wear experiments.

TABLE A2 SINGLE TRAVERSAL WEAR RESULTS, EXPERIMENT 2

Disk	R _a μm	RMS μm	SKEW	KURT	R _t μm	Slope deg.	Peak Curv. μm ⁻¹	Polymer	A _a dia. μm	Load N	Max. Depth μm	Wear Rate μg/m
A11	0.06	0.08	-0.78	5.42	0.59	0.44	-0.009	LDPE PCTFE PVC	564 564 265	0.49 1.96 1.96	0.1 0.1 0.1	0.11 0.49 0.25
B11	0.07	0.08	-0.68	4.39	0.59	0.59	-0.012	LDPE PCTFE PVC	564 564 265	0.49 1.96 1.96	0.1 0.1 0.1	0.25 0.11 0.34
A12	0.06	0.09	-1.02	6.03	0.67	0.55	-0.012	LDPE PCTFE PVC	564 564 265	0.49 1.96 1.96	0.1 0.1 0.1	0.03 0.00 0.00
B12	0.07	0.09	-1.22	6.18	0.61	0.43	-0.009	LDPE PCTFE PVC	564 564 265	0.49 1.96 1.96	0.1 0.1 0.1	0.03 0.32 0.00
A21	0.24	0.31	-0.25	3.33	1.84	1.80	-0.029	LDPE PCTFE PVC	564 564 265	0.49 1.96 1.96	0.5 0.5 0.5	0.51 3.46 3.59
B21	0.22	0.27	0.31	2.96	1.51	1.59	-0.026	LDPE PCTFE PVC	564 564 265	0.49 1.96 1.96	0.5 0.5 0.5	1.16 3.84 2.48
A22	0.21	0.27	-0.05	3.99	1.81	1.78	-0.027	LDPE PCTFE PVC	564 564 265	0.49 1.96 1.96	0.5 0.5 0.5	0.42 2.04 3.98
B22	0.25	0.31	0.04	2.98	1.81	1.71	-0.027	LDPE PCTFE PVC	564 564 265	0.49 1.96 1.96	0.5 0.5 0.5	0.35 3.10 2.46

TABLE A2 (Continued)

Disk	R_a μm	RMS μm	SKEW	KURT	R_t μm	Slope deg.	Peak Curv. μm^{-1}	Polymer	A_a dia. μm	Load N	Max. Depth μm	Wear Rate $\mu\text{g}/\text{m}$
A31	0.88	1.09	-0.21	2.68	5.58	3.69	-0.044	LDPE PCTFE PVC	564 564 265	0.49 1.96 1.96	1.4 1.4 1.4	2.54 17.5 23.7
B31	0.93	1.12	-0.27	2.50	5.86	3.57	-0.044	LDPE PCTFE PVC	564 564 265	0.49 1.96 1.96	1.4 1.4 1.4	2.39 19.7 17.7
A32	0.93	1.13	-0.10	2.79	6.12	3.76	-0.042	LDPE PCTFE PVC	564 564 265	0.49 1.96 1.96	1.4 1.4 1.4	1.42 13.1 24.3
B32	0.91	1.10	-0.46	2.73	5.60	3.52	-0.042	LDPE PCTFE PVC	564 564 265	0.49 1.96 1.96	1.4 1.4 1.4	1.38 20.9 18.4

TEST CONDITIONS, EXPERIMENT 3

Disks were 1018 steel, ground with a unidirectional lay. Surface topography parameters are the averages of four profiles taken perpendicular to the lay. Experiments were performed on a pin-on-disk apparatus. The PVC pins were truncated cones and the diameters of the truncation are tabulated as A_a dia. Wear was determined by mass loss on a microgram balance which had a sensitivity of $\pm 4 \mu\text{g}$. In the experiments a significant change in the apparent area occurred during the run. The A_a dia. is recorded at the beginning and end of the test and the BAR tabulated is the average of the beginning and ending BAR's (which is different from the BAR calculated from the average diameter). On the rough disks 2 or 3 revolutions were sufficient to obtain a wear measurement. Hence several non overlapping spiral wear tracks could be run on one disk. On the smooth disks several revolutions were required to get measurable wear and only one to three measurements could be made on the disk.

The transferred PVC was dissolved off the disks so that replicate experiments could be run. Some disks were cleaned several times and data was obtained on the same surface to obtain a measure of the variability of the wear. Two students obtained the data in Table A3. The properties of the PVC I and II are summarized below.

	PVC I (70000 MW _n)	PVC II (40000 MW _n)
Tensile Strength at Yield, MPa	60.4	60.9
Elongation to Break, m/m	0.66	0.31
Modulus of Elasticity, GPa	3.84	3.88

TABLE A3 SINGLE TRAVERSAL WEAR RESULTS, EXPERIMENT 3

Disk	R _a μm	RMS μm	SKEW	KURT	R _t μm	Polymer	A _a dia. μm Start	End	Load N	BAR Avg.	Wear Rate μg/m	Student
A	1.38	1.71	-0.28	2.85	8.96	PVC I	760	790	19.6	0.23	200	A
							790	840	19.6	0.20	196	
							830	860	19.6	0.19	170	
							620	680	9.8	0.16	20	
							470	560	4.9	0.13	40	
							580	650	9.8	0.16	40	
							510	560	9.8	0.24	53	
							570	600	9.8	0.21	42	
							400	480	4.9	0.17	57	
							500	560	4.9	0.12	43	
							460	520	4.9	0.14	38	
							890	900	9.8	0.087	37	
<hr/>												
							844	901	19.6	0.18	130	D
							901	934	19.6	0.16	142	
							934	971	19.6	0.15	138	
							971	1015	19.6	0.14	105	
							1015	1039	19.6	0.13	119	
							1045	1080	19.6	0.12	107	
							1080	1101	19.6	0.12	104	
							1101	1197	19.6	0.11	103	
							770	852	19.6	0.21	302	
A	1.38	1.71	-0.28	2.85	8.96	PVC II	843	930	19.6	0.18	136	D
							930	981	19.6	0.15	163	
							981	1010	19.6	0.14	121	
							1010	1052	19.6	0.13	154	
							1052	1099	19.6	0.12	161	
							1099	1135	19.6	0.11	116	
							1135	1170	19.6	0.10	133	

* For a given disk and polymer, the horizontal line separates the data taken by students A and D.

TABLE A3 (Continued)

Disk	R _a μm	RMS μm	SKEW	KURT	R _t μm	Polymer	A _a dia. μm Start	End	Load N	BAR Avg.	Wear Rate μg/m	Student	
B	1.70	2.10	-0.36	2.86	10.30	PVC II	770	800	9.8	0.12	35	A	
							800	820	9.8	0.11	10		
							820	850	9.8	0.10	35		
	C	1.27	1.58	0.07	2.76	8.22	PVC I	980	1040	19.6	0.14	140	A
								1040	1100	19.6	0.13	145	
								670	700	4.9	0.07	78	
								910	920	9.8	0.08	33	
								920	950	9.8	0.08	30	
								1100	1170	9.8	0.06	30	
								710	840	19.6	0.23	285	
D	1.27	1.58	0.07	2.76	8.22	PVC II	500	800	19.6	0.35	350	A	
							630	840	19.6	0.26	245		
							830	850	19.6	0.19	145		
							780	880	19.6	0.21	76		
							440	760	19.6	0.40	430		
							580	740	19.6	0.30	480		
							740	820	19.6	0.22	295		
							820	850	19.6	0.20	156		
							850	880	19.6	0.18	230		
							870	880	19.6	0.18	165		
							446	910	19.6	0.43	349		
							475	852	19.6	0.40	211		
							411	899	19.6	0.56	306		
749	901	19.6	0.22	197									
889	1010	19.6	0.16	127									
996	1038	19.6	0.13	107									
795	937	19.6	0.19	195									

TABLE A3 (Continued)

Disk	R _a μm	RMS μm	SKEW	KURT	R _t μm	Polymer	A _a dia. μm	End	Load N	BAR Avg.	Wear Rate μg/m	Student
C	1.27	1.58	0.07	2.76	8.22	PVC I	470	660	19.6	0.38	400	A
							440	680	19.6	0.40	390	
							520	730	19.6	0.36	310	
							660	740	19.6	0.30	170	
							600	720	19.6	0.32	250	
							590	720	19.6	0.31	450	
							560	730	19.6	0.35	215	
							840	890	19.6	0.19	80	
							820	860	19.6	0.20	135	
MA	0.30	0.37	-0.78	4.93	2.60	PVC I	490	650	19.6	0.38	35	A
							460	680	19.6	0.40	26	
							810	830	19.6	0.20	8.7	
MB	0.27	0.34	-0.66	3.69	2.01	PVC I	830	830	9.8	0.10	2.9	A
							748	771	19.6	0.24	14	D
							771	783	19.6	0.23	13	
							646	746	19.6	0.29	37	
							746	751	19.6	0.25	34	
							635	705	19.6	0.33	25	
							705	730	19.6	0.30	32	
							730	743	19.6	0.28	15	
							743	767	19.6	0.24	28	
							751	829	29.4	0.34	44	A

TABLE A3 (Continued)

Disk	R_a μm	RMS μm	SKEW	KURT	R_t μm	Polymer	A_a dia. μm	Start	End	Load N	BAR Avg.	Wear Rate $\mu\text{g}/\text{m}$	Student
MB	0.27	0.34	-0.66	3.69	2.01	PVC II	972	985	19.6	0.14	14	D	
								874	19.6	0.18	32		
								741	19.6	0.24	21		
								791	19.6	0.22	11		
								707	19.6	0.26	29		
761	19.6	0.23	27										
MC	0.26	0.33	-0.80	4.17	1.94	PVC I	787	827	29.4	0.32	56	A	
							827	871	29.4	0.29	89		
MD	0.30	0.39	-0.78	3.76	2.38	PVC I	420	700	19.6	0.42	18	A	
							660	730	19.6	0.28	8.7		
ME	0.26	0.33	-0.50	3.13	1.85	PVC I	810	860	19.6	0.19	12	A	
							820	830	9.8	0.11	2.9		
						PVC I	660	730	19.6	0.28	10	A	
							PVC II	454	785	19.6	0.45	70	D
								785	806	19.6	0.22	40	
								460	765	19.6	0.45	58	
								747	781	19.6	0.24	40	
								664	738	19.6	0.28	32	
							PVC I	464	660	19.6	0.48	68	D
								665	717	19.6	0.29	16	
								717	750	19.6	0.26	17	
								750	762	19.6	0.24	13	
762	776	19.6	0.24	15									

APPENDIX B

A model for the Abrasive Wear of Polymers

[Based in part on a dissertation by J. H. Herold submitted to VPI&SU in partial fulfillment of requirements for the degree of Doctor of Philosophy, June 1980]

ABSTRACT

A model for the abrasive wear of polymers is developed. The model uses digitized profile data from the abrading surface, the mechanical properties of the polymers, and the applied load. The ability of the model to calculate the filling of void volumes on the surface gives the model the capability of predicting a reduction in wear rate for repeated traversals over an abrading surface, of predicting the change in wear rate with sliding direction on pins with noncircular cross-section, and of predicting the change in wear rate as a function of bearing area ratio.

NOMENCLATURE

- A_a = apparent area of contact
 A_r = real area of contact
 b = length of a wear particle
 c = proportionality constant
 d = sliding distance
 D = slider width
 e = cross section area of void space
 E = volume of void space
 f = cross section area of wear particle
 F = accumulated volume of wear particles
 G = particle formation rate factor
 h = height of a wear particle
 k = wear coefficient
 L = profile length
 n = number of penetrating asperities
 N = number of asperities producing wear particles
 p = penetration depth (maximum if unsubscripted)
 P_m = flow pressure
 R = radius of a circular track
 R_a = arithmetic average roughness
 S = slider length
 T_g = glass transition temperature
 V = total wear volume
 W = normal load

Y = yield strength of polymer in tension

Z = number of repeated traversals

ϵ = elongation to rupture

θ = slope of the asperity

ϕ = polymer deposit angle

Subscripts

i = values at the i^{th} asperity

INTRODUCTION

Abrasive wear occurs when a hard, sharp particle cuts or displaces material from the polymer. The simplest form of abrasive wear occurs during single traversal sliding (the slider is continuously exposed to new surface). In single traversal sliding the wear of the polymer is a direct response to the interaction of the hard surface topography and the polymer properties.

Most single traversal sliding experiments are performed at the sliding speeds less than 1 cm/s to avoid heating the polymer and changing its mechanical properties. Investigators have correlated wear in single traversal sliding with polymer properties such as the inverse of the product of the stress and elongation at rupture [1-3]¹, the cohesive energy [4], the flexure modulus, and the inverse of the yield strain [5]. Investigators have also correlated single traversal wear with surface topography features such as the average slope of the asperities and the arithmetic average roughness R_a [2,6], and the ratio of the standard deviation of the asperity heights to the average radius of the asperities [7].

Models of single traversal abrasive wear incorporate the polymer properties and the topography of the hard surface or parameters derived from the surface profiles. A model based on derived surfaces parameters is expressed by Eq. 1.

$$V = kWd \overline{\tan \theta} / p_m \quad (1)$$

where V is the wear volume, k is a constant which accounts for that

¹Numbers in brackets designate References at the end of the paper.

fraction of the deformed material which is removed from the system, W is the normal load, d is the sliding distance, $\tan \theta$ is the average slope of the asperities, and p_m is the flow pressure of the polymer [2,8]. However, the linear relation between V and $\tan \theta$ has not been experimentally verified. The wear, V , was found to be proportional to $\tan \theta$ to a power greater than one [2,6]. In general, a model such as that expressed by Eq. 1 contains a constant which must be evaluated for each polymer in a wear experiment.

A wear model, based on the computer profile information, identified asperities which penetrated the polymer and then calculated the polymer wear at each asperity by assuming that the wear particles were wedge shaped [9]. The volume of wear is expressed by Eq. 2.

$$V = d \sum_{i=1}^n p_i^2 D / (2L \tan \phi) \quad (2)$$

where p_i is the depth of penetration of the i^{th} asperity into the polymer, D is the width of the polymer slider, L is the length of the surface sampled, and ϕ is the deposit angle of the transferred polymer as measured by Warren [3].

The deposit angle was shown to be proportional to the inverse of the energy to rupture for a given polymer. The major improvement of the model expressed by Eq. 2 over that given by Eq. 1, is that no experimentally determined wear coefficient is needed to evaluate Eq. 2. The wear of three polymers, polyvinyl chloride (PVC), low density polyethylene (LDPE), and polychlorotrifluoroethylene (PCTFE) were predicted to

within a factor of five of measured wear over a range of bearing area ratios (BAR) from 0.1 to 0.3.

There were several assumptions made in the model expressed by Eq. 2 which were responsible for the limited range of BAR over which predictions were in best agreement with experiments.

1. Every asperity which penetrated the polymer produced a wedge-shaped wear particle.
2. There was only one wear particle produced regardless of the length of polymer which slid past the asperity.
3. The volume of the wedge was a function of only the penetration depth of the asperity into the polymer and the deposit angle.
4. The wedge was produced regardless of the availability of space for the particle to reside in the region between the polymer and metal surfaces.

The major purpose of the work reported in this paper is to develop a new model in which the above assumptions are relaxed. An experimental study is described in which the shape and rate of generation of polymer debris particles was observed. The description of the model is followed by its mathematical formulations.

OBSERVATIONS OF WEAR PARTICLE FORMATION

When the transfer of polymer to an abrading surface occurs the geometry of the transferred material and the frequency at which it transfers is a function of the polymer properties and the surface topography. If the abrading surface is a ground surface, the effect of the

randomness of the surface features is confounded with the effect of the variability of the response of the polymer in determining wear. To isolate the latter effect, an experiment was performed in which the abrading surface consisted of parallel ridges of the same geometry.

The surface was of a triangular form with 45 deg. flank angles as shown in cross section in Fig. B1. The surface was made up of 200 sheets of 25.4 μm thick stainless steel which were clamped to the appropriate angle in an apparatus. This geometry provided a peak-to-peak spacing of 36 μm with an R_a of 4.5 μm .

Six polymers, PVC, PCTFE, Nylon 6-6, LDPE, polytetrafluoroethylene (PTFE), and polyoxymethylene (POM) were fabricated into pins which were truncated cones. The pins were traversed across the abrading surface at approximately 1.0 cm/min. The normal loads were selected to result in a $\text{BAR} \approx 0.1$.

All the experiments were carried out under ambient laboratory conditions, the ambient temperature being about 24°C. At this temperature, PVC, PCTFE, and Nylon 6-6 were well below their glass transition temperatures, T_g 's, 87, 45, and 50 C respectively, a state referred to as glassy. PTFE, LDPE, and POM were tested above their T_g 's, -50, -126, and -50 C respectively [10]

The three polymers tested at temperatures below their T_g 's all exhibit the similar phenomenon of discrete, uniform sized wear debris. The PCTFE debris of Fig. B2 is a particularly good example of the discrete polymer wear process which was found to be characteristic of the wear of glassy polymers. The top of this photograph represents the

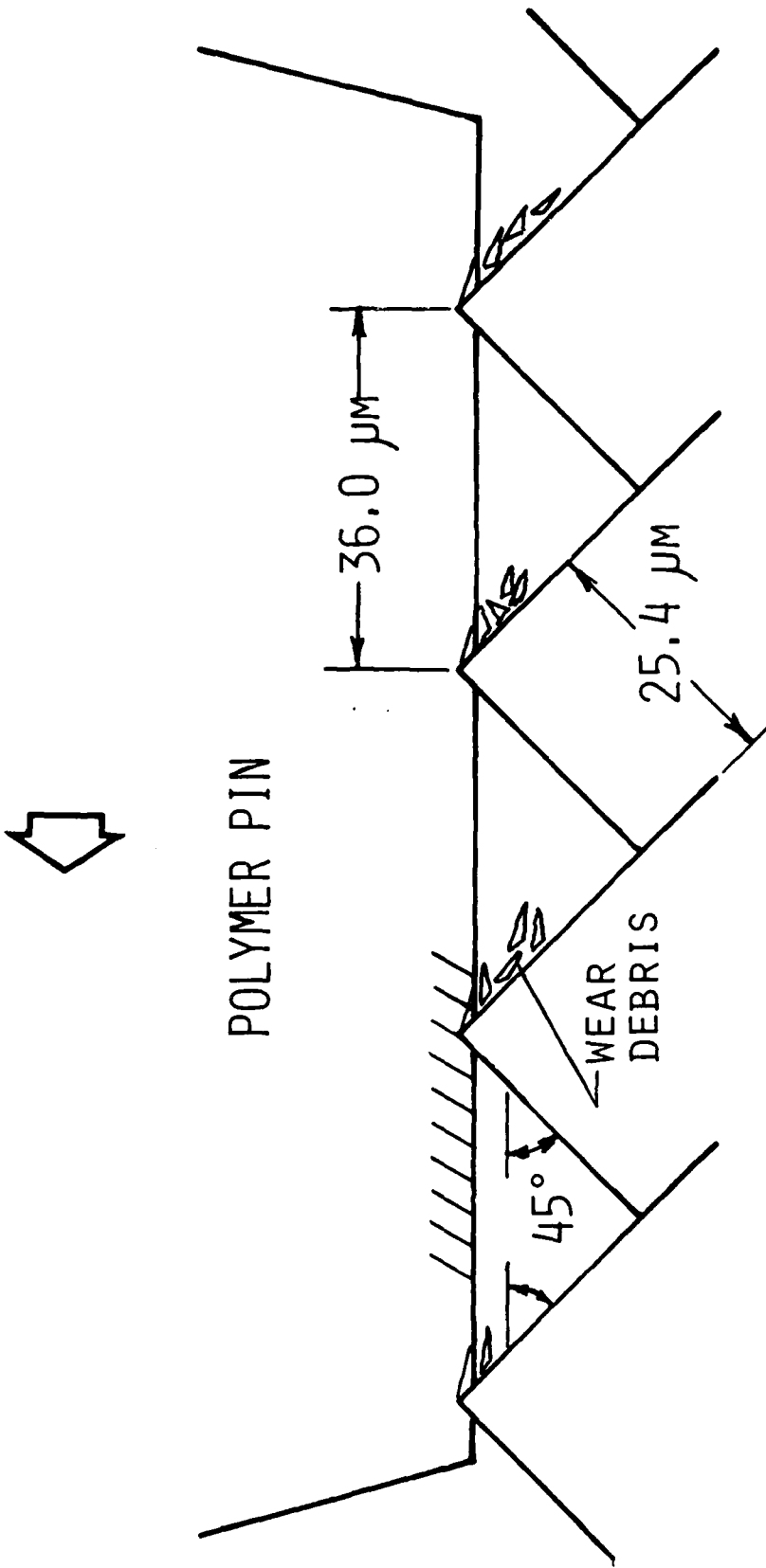


Figure B1. Cross section of a deterministic surface



Figure B2. PCTFE wear particles on a deterministic surface

region near the edge of the polymer pin prior to sliding. The increasing amount of debris in the grooves toward the bottom of the photograph was a result of the lower ridges having more sliding contact with the polymer than the upper ridges. The important feature of the debris is its discrete, lumpy form. It is this wear in discrete lumps, idealized as wedges, that this wear model will attempt to simulate.

The LDPE of Fig. B3 and the PTFE of Fig. B4 exhibit drawing of the polymer into sheets and strands respectively. It is obvious that these polymers, tested above their T_g 's, do not exhibit the characteristic mode of wear of glassy polymers. For this reason, the model of abrasive wear described in this paper is applicable only to the wear of glassy polymers.

WEAR MODEL

The wear model is based on the following sequence of events. First, the normal load causes some of the asperities on the rigid surface to penetrate the polymer until the real area of contact is sufficient to support the load. Second, some of the penetrating asperities will produce wear particles when tangential motion occurs. Third, wear particles are produced until the volume of space adjacent to each of these asperities is filled with wear particles. The models for such of these events are discussed in the following sections.

Penetration Depth

When a normal load W was applied to the polymer, the asperities of the abrading surface penetrated the polymer until the real area of contact A_r was sufficient to support the load. The relation between A_r and W was given by $A_r = W/p_m$, the flow pressure, was assumed to be



Figure B3. LDPF wear deposits on a deterministic surface



Figure B4. PTFE wear deposits on a deterministic surface

constant and equal to three times the yield strength Y of the polymer in tension [11].

The A_r is usually less than the apparent area of contact A_a which defines the maximum value of A_r . The ratio A_r/A_a is the BAR which was given by

$$\text{BAR} = W/3YA_a \quad (3)$$

For an ideally flat polymer surface and a given normal load the asperities of the rough surface penetrated to depth p_i at which the A_r was sufficient to support the load. The relationship between the real area of contact and the penetration depth, p , of the highest asperity is a statistical height parameter of the rough surface which is called the bearing area curve (BAC). Therefore, given a BAR value and the BAC for the metal surface, the penetration depth, p , of the highest asperity can be determined. Figure B5 shows three BAC's for ground steel surfaces, each of a different roughness.

In the wear model, the BAR was calculated using Eq. 3. Thus, the normal load, polymer yield strength in tension, and the apparent area of contact were inputs to the model. The BAC was calculated from digitized profiles of the rough surface. The BAR and the BAC determined the penetration depth, p . Then, the profile was searched and all penetrating asperities were identified and their penetration depths p_i were calculated.

Geometry of Wear Particles

There are two necessary conditions for the generation of wear debris. First, the asperity must penetrate the polymer. Second, of that portion of the asperity penetrating the polymer, the cutting side

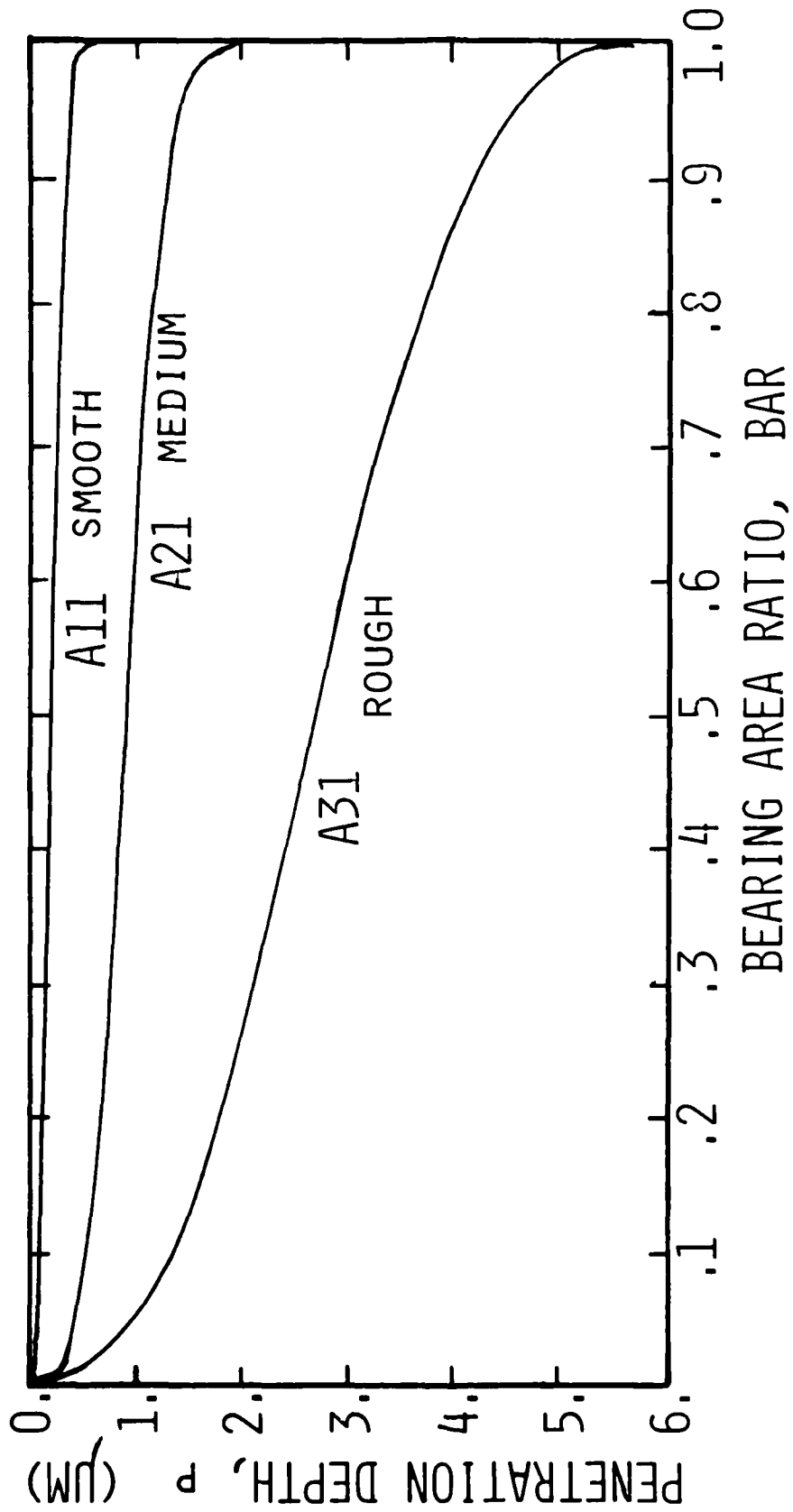


Figure B5. Typical bearing area curves for abrading surfaces

must have a slope, θ , greater than the deposit angle ϕ for the polymer. Therefore, unless the slope of the asperity at its peak is greater than the deposit angle, the height of the wear particle h_i will be less than the penetration of depth p_i as shown in Fig. B6.

In this model it was assumed that a rectangular cross-section, polymer pin slid over an abrading surface which consisted of parallel ridges. The sliding direction was assumed perpendicular to the direction of the ridges. Hence, the asperity shown in Fig. B6 is the cross section of a ridge. The area of the wear particle is f_i . The volume of the wear particle is the area f_i multiplied by the pin dimension D perpendicular to the sliding direction.

The implementation of this part of the wear model by the computer is as follows. For each penetrating asperity identified in the previous section, the asperity slopes were calculated at successive points. When the slope exceeded the deposit angle for the polymer the wedge area f_i was calculated by numerical integration. The wedge volume was calculated by Df_i .

Wear Particle Formation Rate

To aid in understanding this section, five terms related to length and distance will be defined. The sliding distance d is the total displacement of the slider relative to the abrading surface. The profile length L is the length on the abrading surface which was sampled with a profilometer to obtain the profile data. The wear particle length b_i is defined in Fig. B6. The slider width D is the dimension of the slider perpendicular to the sliding direction. The slider length S is the dimension of the slider parallel to the sliding direction.

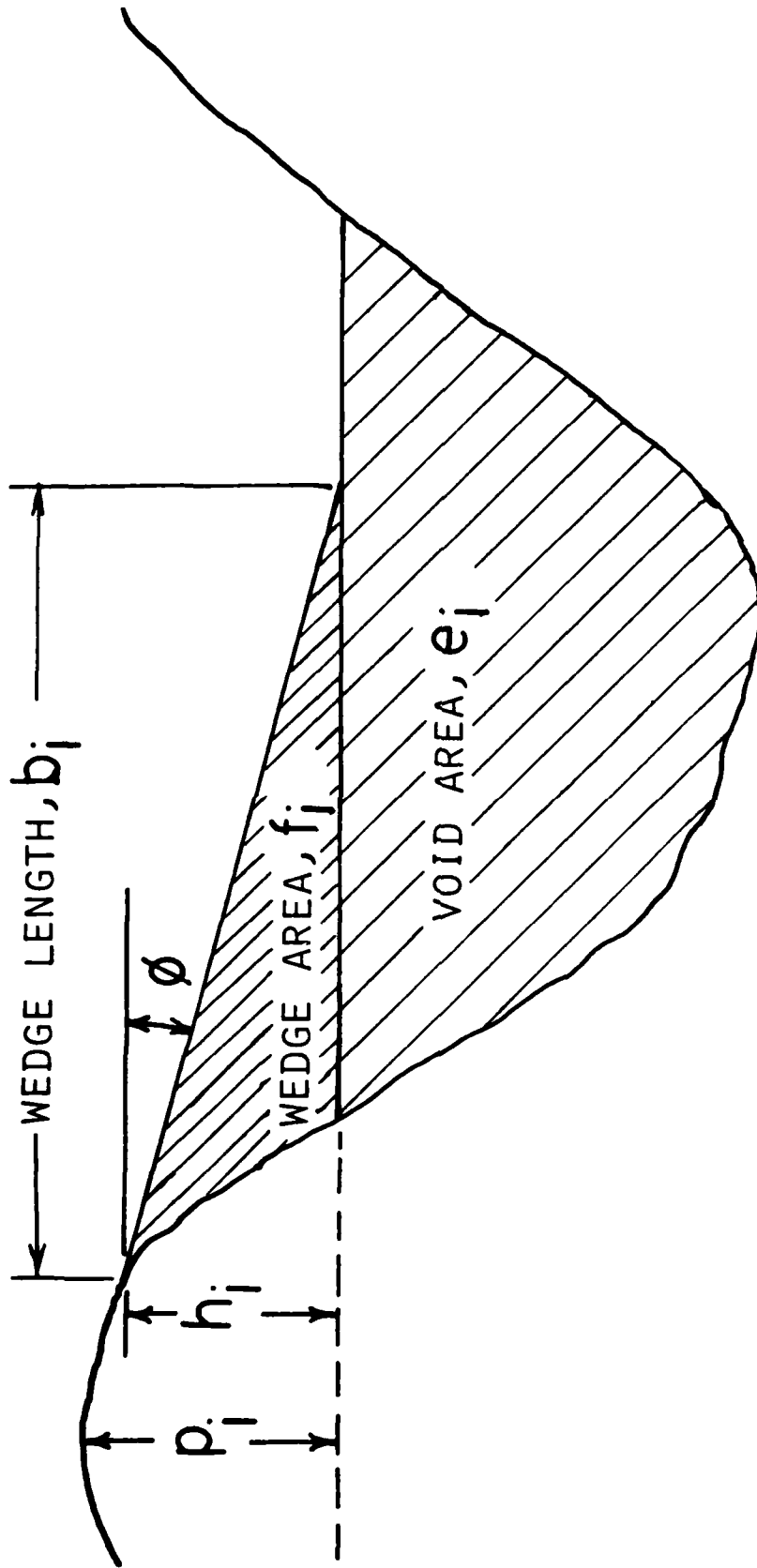


Figure B6. Cross section of wear particle and void space

The wear particle formation rate is a function of the sliding distance necessary to produce a wear particle at a given asperity. This sliding distance was defined as the product $b_i G \epsilon$ where ϵ is the elongation to rupture of the polymer and G is a constant. The length of the wedge was included in this product because short wedges should be generated more frequently than long wedges. This statement is equivalent to stating that the number of wear particles which can be generated in a given sliding distance is larger for small particles than for large wear particles.

The ϵ was included in this product to permit the wear rate to reflect the dependence of polymer wear on ϵ observed by other researchers. Ratner et al. [1] state "...the act of wear as a separation of particles occurs only when the elongation brought about by the abrasion exceeds the breaking elongation of the material..." The constant G must be determined by an iterative procedure in which different values of G are assumed until the predicted and measured wear rates agree. These calculated values of G for PVC and PCTFE are compared in a later section.

In a single traversal wear test, the maximum length of polymer that an asperity encounters is the slider length S . In a multiple traversal wear test, the maximum length of polymer that an asperity encounters is ZS where Z is the number of repeated traversals. In this model, it is assumed that wear particles are produced until the wear particle volume exceeds the void volume adjacent to the asperity. If the total volume of wear particles is less than the adjacent void volume then the number of wear particles produced is given by $ZS/b_i G \epsilon$.

The computer implementation of the wear particle formation rate required a calculation of the void volume immediately adjacent to the asperity as well as the wear wedge volume. The computer summed the wedge volumes produced for the given sliding distance. When the accumulated wedge volume equaled or exceeded the void volume associated with the asperity, the wear associated with the asperity was set equal to the void volume. If the sliding distance was less than that necessary to fill the void volume then the wear at that asperity was the accumulated wedge volume.

Mathematical Formulation of the Wear Model

The wear volume for the i^{th} asperity, V_i , is the smaller of the void volume E_i and the accumulated volume of wear particles F_i .

$$V_i = \min(E_i, F_i) \quad (4)$$

The void volume E_i is given by:

$$E_i = De_i \quad (5)$$

Where e_i is the void area adjacent to the i^{th} asperity as shown in Fig. B6. The accumulated volume of wear particles F_i for a single traversal ($Z=1$) is given by:

$$F_i = (S/Gb_i \epsilon)(Df_i) \quad (6)$$

where the term in the first parentheses is the number of particles and the term in the second parentheses is the volume of one particle. The total wear volume is given as:

$$V = (d/L) \sum_{i=1}^N V_i \quad (7)$$

where d/L is the ratio of the total sliding distance to the sampled portion of that distance and N is the number of asperities producing wear particles in the profile sample length L .

MODEL GENERALIZATION

In the wear model expressed by Eqs. 4-7 the polymer pin was assumed to have a rectangular cross section. Additionally it was assumed that the polymer was traversed in a direction normal to the lay of a ground surface. In the following sections the model was generalized to include sliding in directions not perpendicular to the lay direction and polymer pins with a circular cross section.

Sliding Direction Relative to Lay

For a sliding direction at a diagonal to the lay of a counterface it was assumed that only the component of motion perpendicular to the lay contributed to the wear of the polymer. Thus, if a polymer slid across a surface with a lay, the sliding distance d used in the model was the actual sliding distance times the cosine of the angle between the sliding direction and the normal to the lay direction. In traversing a circular path of radius R , on a disk with unidirectional lay, the polymer pin travels a distance of $2\pi R$. However, the total distance traveled by the polymer in a direction normal to the lay is two diameters, $2(2R) = 4R$. For one complete disk revolution, the ratio of the normal distance traveled to the actual distance traveled was $4R/2\pi R = 2/\pi$. Therefore, the modeled wear based on the actual distance traveled must be multiplied by $2/\pi$ if the wear occurs on a disk with unidirectional lay.

Surfaces that are machined with a lay have roughness in a direction parallel to the lay. Thus, wear will occur when sliding parallel to lay and the above assumption will result in an underprediction of wear.

When wear occurs on a rotating unidirectionally ground disk, the sliding direction is parallel to the lay for an infinitesimal sliding distance twice per revolution. Thus, the assumption that no wear occurs when sliding parallel to the lay should cause an insignificant error in the wear prediction.

Pin Geometry

The model input most dependent on the geometry of the pin is the slider length. For the rectangular cross section slider, the slider length is constant over the entire width D of the slider. However, for a slider with a circular cross section the slider length varies from zero at either edge of the slider to a value equal to the pin diameter at the center of the slider.

Figure B7 illustrates the effect of slider length on simulated wear. Each of the two bands shown represents a 95% confidence interval for the mean wear predicted for sixteen different profiles. There were four disks used for each roughness; and four profiles were taken from each disk. The asymptotic behavior of the predicted wear was attributed to the successive filling up of some of the void regions. When a void was full, the adjacent asperity no longer contributed to the wear of the polymer. When the slider length was extended to large values, all the voids eventually filled. This condition signaled the termination of the transient stage of abrasive polymer wear.

One method for modeling a circular pin was to approximate the circle with several rectangles of constant width and variable slider length. However, to reduce the computation time, the circular pins were modeled as rectangular pins with a width D equal to the pin diameter and

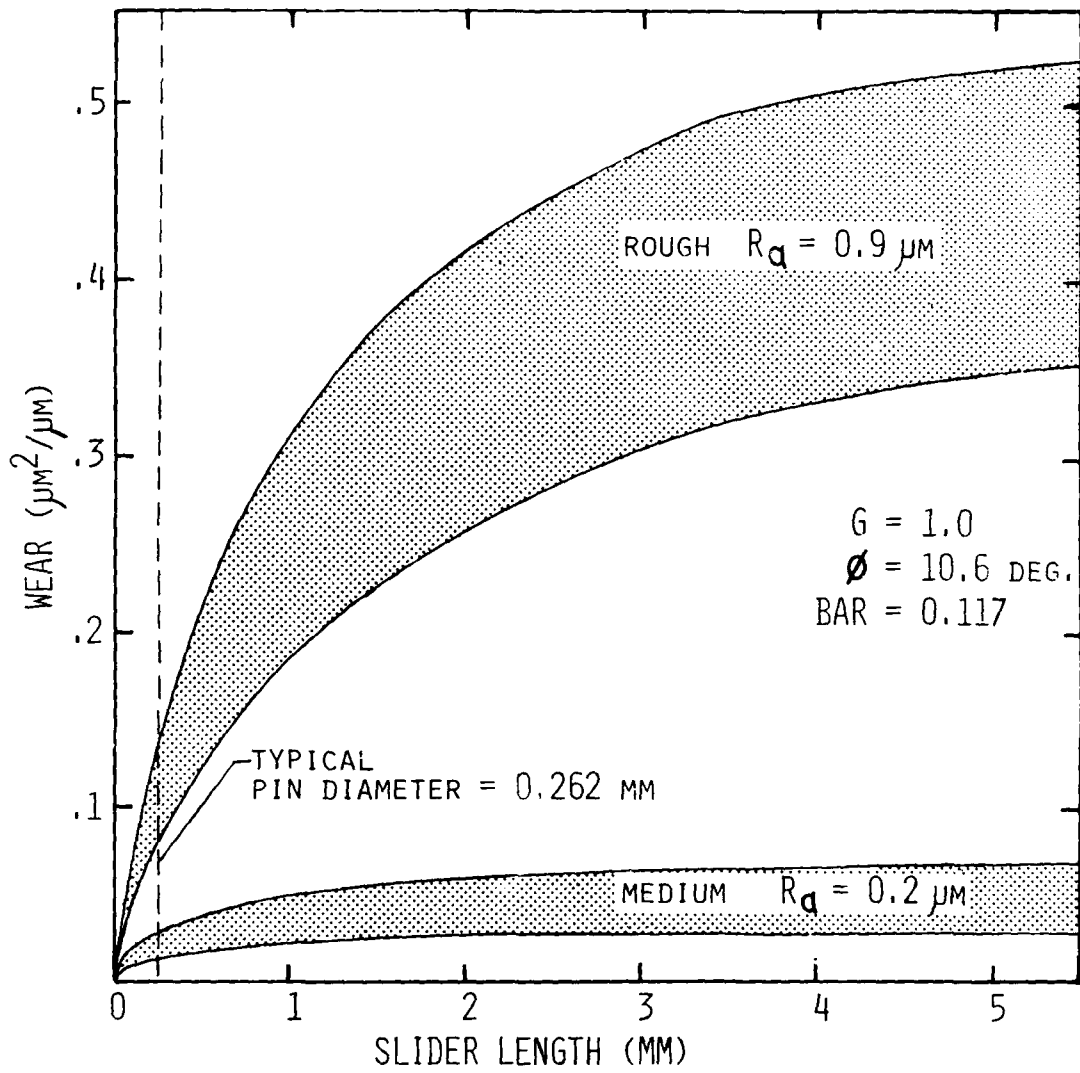


Figure B7. Modelled wear as a function of slide length for medium and rough surfaces. The bands are the 95 percent confidence interval for the mean of 16 profiles.

a length S equal to $\pi/4$ times the pin diameter. Thus, the area of the rectangular pin was the same as that of the circular pin.

There were two methods of incorporating this pin correction factor in the wear model. In the first method the diameter of the pin was multiplied by the pin correction factor prior to inputting this dimension into the model as the slider length. Thus, the slider length was given by

$$S = \pi D/4 \quad (8)$$

When Eq. 8 was substituted into Eq. 6, the accumulated wedge volume became:

$$F_i = \left[\frac{\pi D}{4 G b_i \epsilon} \right] (D f_i) = \frac{\pi D^2 f_i}{4 G b_i \epsilon} \quad (9)$$

In the second method the pin diameter was set equal to the slider length, $S = D$. Thus Eq. 6 became

$$F_i = \left[\frac{D}{G b_i \epsilon} \right] (D f_i) = \frac{D^2 f_i}{G b_i \epsilon} \quad (10)$$

In this case the resulting modeled wear was then multiplied by the pin correction factor.

$$V = \frac{\pi}{4} \frac{d}{L} \sum_{i=1}^N V_i \quad (11)$$

If the second method was used and the model calculated that none of the voids were full, the two methods of correcting for pin geometry were equivalent. They both predicted the same wear that would have been predicted by modeling the pin as several rectangular slabs.

If the first method was used and the model calculated that some or all of the voids were full, the first method of correction overpredicted wear, while the second method underpredicted wear. The difference in the wear predicted by the two correction methods seldom exceeded ten per cent for any of the predicted wear rates for an assumed value of $G = 1.0$. It is interesting to note that when the second method was used, the pin correction factor was applied in a manner identical to the lay correction of the previous section, forming a combined factor of $(2/\pi)(\pi/4) = 0.5$.

CALCULATION OF THE G FACTOR

The experimental data used to calculate the G factor were reported in Ref. 12 and are reproduced in Table A2 in Appendix A of this report. Because the wear model did not correspond to the transfer mode of LDPE, only the data for PVC and PCTFE were used to calculate G. Since the wear data were obtained with pins having circular cross sections sliding on disks with a unidirectional lay the following equation was used to calculate the G factor:

$$V = 0.5 (d/L) \sum_{i=1}^N V_i \quad (12)$$

where v is given by Eq. 4, E_i by Eq. 5, and F_i by Eq. 10 and V is the measured wear. The values of ϵ used were 0.26 for PVC and 1.25 for PCTFE. The values of G given in Table B1 were calculated by an iterative procedure in which successive values of G were assumed until the predicted wear equalled the measured wear.

The values found for G had the following relationships. For PVC, the variance in G was small within a given roughness level and there was

Table B1 Wear Rates and G Factors

Disk	Polymer				
	R_a (μm)	PVC ($\rho = 1.35 \text{ g/cc}$) $\phi = 10.6^\circ, \epsilon = 0.26$		PCTFE ($\rho = 2.2 \text{ g/cc}$) $\phi = 12.8^\circ, \epsilon = 1.25$	
		Wear Rate (mm^3/km)	G	Wear Rate (mm^3/km)	G
A21	0.24	2.66	10.6	1.57	18.
B21	0.22	1.84	12.2	1.75	9.6
A22	0.21	2.95	13.3	0.93	36.8
B22	0.25	1.82	11.8	1.41	10.4
A31	0.88	17.56	6.5	7.95	15.2
B31	0.93	13.11	9.9	8.95	16.0
A32	0.93	18.00	6.6	5.95	30.4
B32	0.91	13.63	6.5	9.50	9.6

a significant difference between the mean values of G for the surfaces with R_a equal to 0.2 and 0.9 μm . The variance in G was large within a given roughness level for PCTFE and there was no significant difference between the values of G at different roughnesses. The cause of the large variance in the values of G for PCTFE were the low wear rates measured on disks A22 and B32. It should be noted that the wear rate varies inversely with G . For a low wear rate, the model requires that the amount of sliding necessary to produce a wear particle be large and G is the factor which determines this sliding distance.

Because wear was measured for each polymer on each disk, the values for G for each polymer on the same disk were compared using the Wilcoxon Signed-Rank Test to determine if there was a significant difference. The test indicated that the probability that the values of G were significantly different for the two polymers was 0.96.

DISCUSSION

The results indicated that the values of G are significantly different for each polymer. If the values of G had been the same for each polymer then the conclusion could be made that the factors included in the model related to the polymer properties, i.e. the deposit angle ϕ , the yield strength Y , and the elongation to rupture ϵ were sufficient to predict the measured differences in wear rates. Thus, the significantly different values of G imply that the model has not modeled the polymer properties correctly. Therefore, the assumptions made in the model will be examined more critically in the following paragraphs.

The polymer flow pressure, p_m , is central to the penetration phase of the model. It was taken to be three times the yield stress in tension. No consideration was given to strain rate dependencies, strain hardening, additional interfacial pressure components contributed by friction and tangential cutting forces, or distortion of the contact area due to tangential forces, viscoelastic deformations, or material removal. The effect of possible load support by polymer wear debris trapped in filled void regions was also neglected.

When the accumulated wear particle volume equaled the void volume next to a penetrating asperity, it was assumed that no more wear particles were produced by that asperity and that no other asperities were affected by this occurrence. However, if part of the normal load was carried by the polymer debris, then less load will be carried by the metal asperities. Because penetration decreased as the load carried decreased, the predicted wear would decrease if the model included load support by the filled void volumes.

The effect of the geometry of an indenter on the value of c in the relationship $p_m = cY$ where Y is the yield strength in tension of the indented material has been investigated [13,14]. For a perfectly rigid-plastic material indented by a rather blunt indenter, $c = 3.0$ [15]. For elasto-plastic materials, c is given by a more complex relationship [16] in which c can have values less than 3.0 for blunt wedges. Most polymers have elasto-plastic behavior and therefore could have values of $c < 3.0$. However, it would require an entirely separate investigation to determine how to model a randomly shaped asperity as a wedge with a constant slope so that the theoretical predictions of c as a function of the wedge angle could be included in the penetration part of the wear model. Therefore, the value of c was set equal to 3.0 for this wear model.

The polymer deposit angle, ϕ , is central to the section of the model which determines the geometry of wear particles. This deposit angle was based on the measurement of the average angle of polymer deposits [3]. Modeling a complex failure zone in the polymer as a singular angle is doubtless an oversimplification of the event leading to the production of a wear particle. It does, however, yield a model in which the wear predicted at an asperity is functionally related to the slope of the asperity. Indeed it is this parameter which determines whether or not a penetrating asperity will generate a wear particle.

One consequence of the assumption of a constant deposit angle in the model was that on the smooth surfaces in 75 per cent of the predictions no wear was calculated, which implied that none of the penetrating asperities had slopes greater than the deposit angle. The fact

that wear was measured on some of these surfaces could have resulted from asperities with slopes less than the deposit angle removing polymer. It is also possible that the finite radius on the stylus used to generate surface profiles filtered out features of the surface which caused polymer transfer to occur. A third possibility is that some adhesive transfer occurred.

One unique feature of the model is its ability to terminate the production of wear particles at an asperity when the associated void volume has been filled. This feature makes it possible for the model to predict a decreasing wear rate as the slider length increases. This prediction is illustrated in Fig. B7 (the slope of the wear curve is the wear rate). This prediction of decreasing wear rate by the model is analogous to the observed decrease in the cutting rate of a file as the grooves become clogged with wear debris.

This feature also gives the model the capability of predicting different amounts of wear for different directions of sliding on a noncircular apparent area of contact. This phenomenon has been observed by Lancaster [17] in single traverse experiments. For sliders with a rectangular apparent areas of contact, higher wear was measured when the sliding direction was parallel to the short side than when the sliding direction was parallel to the long side. The reason for this difference is the filling of the voids with debris. When sliding parallel to the short side, fewer void volumes fill up with debris than when sliding parallel to the long side. Hence, higher wear occurs when sliding parallel to the short side.

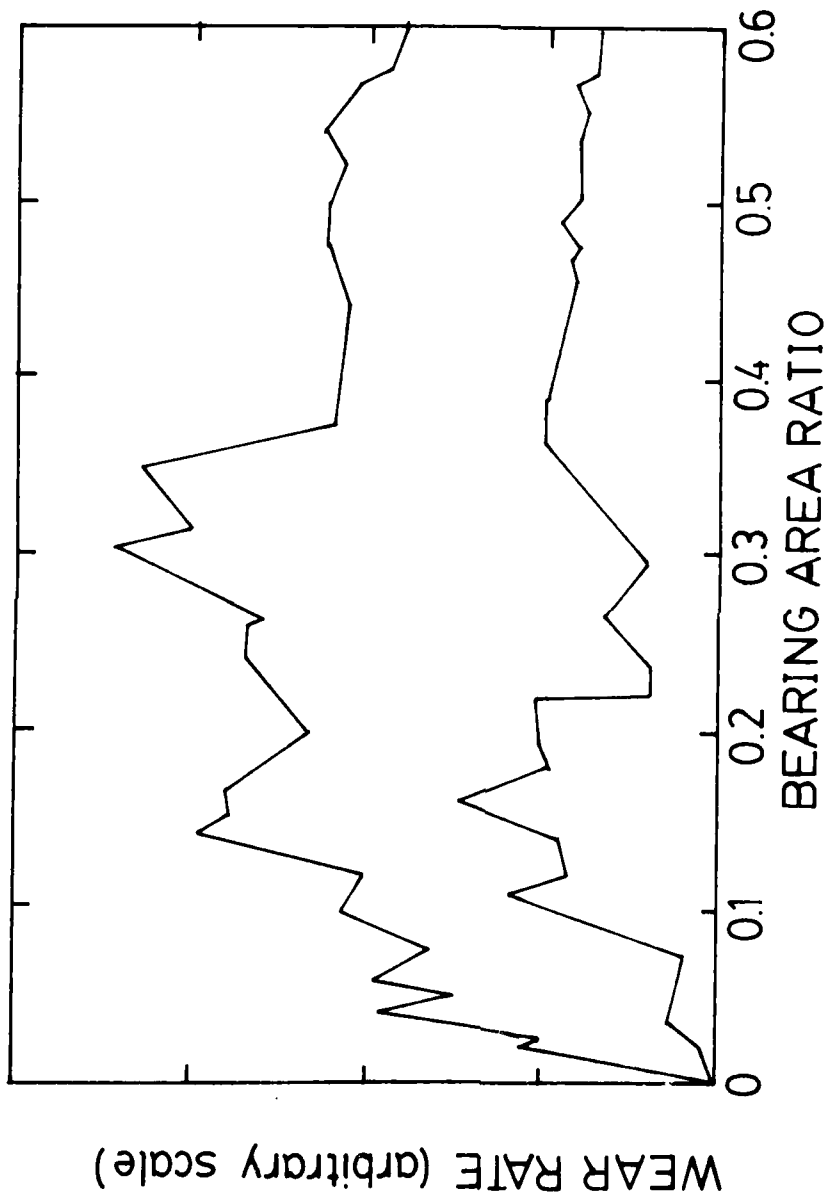


Figure 36. wear rate as a function of Bearing Area Rat

In the model, this experiment is simulated by exchanging the values for S and D in Eqs. 5 and 6. Note that only D occurs in the equation for void volume E_i while both S and D occur in the equation for the accumulated volume of wedges F_i . Hence, exchanging the values of S and D will change E_i but not F_i . If D has the smaller value, then sliding is parallel to the long side of the rectangle. If D is smaller, then E_i is smaller and V_i is determined by E_i rather than F_i for more asperities. Hence the calculated wear volume will be smaller which is in agreement with Lancaster's observations.

The model also has the capability of predicting wear rate as a function of changes in the BAR. Such a plot is shown in Figure B8. The upper and lower curves represent the envelop of the wear rate predictions for four profiles from a given disk. The wear rate predictions increased as the BAR increased from 0 to 0.3 after which they decreased slowly as the BAR increased from 0.3 to 0.6. The reason for this behavior is that as the BAR increased, the polymer surface was more deeply penetrated by the asperities. The void space between the contacting asperities decreased. Thus, when sliding was simulated and wear particles were produced, there was less void volume for the accumulation of particles and hence less wear produced.

This prediction has been confirmed experimentally. The data plotted in Fig. 2 are for the same disk as was used in the simulated wear plotted in Fig. B8. In Fig. 2 it is also noted that the wear rate reached a peak between BAR's of 0.3 and 0.4 and then decreased at larger values of BAR.

CONCLUSIONS

The model has the capability of monitoring the amount of filling of the surface by debris particles. This feature permits the model to predict the following:

1. The decrease in wear rate for repeated sliding over a surface,
2. The variation in wear rate as a function of sliding direction for sliders with noncircular apparent areas of contact, and
3. The variation in wear rate as a function of BAR.

However, the model does not have the capability of predicting wear given polymer properties, surface roughness, and the normal load. Hence, additional work is needed to discover the combination of the above input data which will correctly predict wear.

REFERENCES

1. Ratner, S. B., Farberova, I. I., Radyerkevich, O. V. and Lur'e, E. G., "Connection between Wear-Resistance of Plastics and Other Mechanical Properties," in Abrasion of Rubber, Ed. James, D. S., MacLaren, London, 1967, p. 145.
2. Lancaster, J., "Abrasive Wear of Polymers," Wear, Vol. 14, 233, 1969.
3. Warren, J. H. and Eiss, N. S., "Depth of Penetration as a Predictor of the Wear of Polymers on Hard, Rough Surfaces," Trans. ASME, Jl. Lub. Tech., Vol. 100, January 1978, pp. 92-97.
4. Giltrow, J. P., "A Relation Between Abrasive Wear and the Cohesive Energy of Materials," Wear, Vol. 15, 1970, p. 71.
5. Lontz, J. F. and Kumnick, M. C., "Wear Studies of Moldings of Polytetrafluorethylene Resin, Considerations of Crystallinity and Graphite Content," ASLE Trans., Vol. 16, 1973, p. 276.
6. Eiss, N. S. and Warren, J. H., "The Effect of Surface Finish on the Friction and Wear of PCTFE Plastic on Mild Steel," Soc. Manufacturing Eng., Paper No. IQ75-125.
7. Hollander, A. E. and Lancaster, J. K., "An Application of Topographical Analysis to the Wear of Polymers," Wear, Vol. 25, 1973, p. 155.
8. Rabinowicz, E., Friction and Wear of Materials, John Wiley and Sons, Inc., New York, 1965, p. 168.
9. Eiss, N. S., Jr., Wood, K. C., Smyth, K. A. and Herold, J. H., "Model for the Transfer of Polymers on Hard, Rough Surfaces," Trans. ASME, Jl. Lub. Tech., Vol. 101, April 1979, pp. 212-218.
10. Steijn, R. P., "Friction and Wear of Plastics," Metals Engineering Quarterly, Vol. 7, No. 2, American Society for Metals, May 1967, pp. 9-21.
11. Bowden, F. P., and D. Tabor, The Friction and Lubrication of Solids, Part I, Oxford University Press, Elv House, London, 1950, pp. 10-14.
12. Eiss, N. S., Jr. and Smyth, K. A., "The Wear of Polymers Sliding on Polymeric Films Deposited on Rough Surfaces," ASME Paper No. 80-C2/Lub-24.

13. Bowden, F. P., and D. Tabor, The Friction and Lubrication of Solids, Part II. Oxford Clarendon Press, 1964, p. 333.
14. Hill, R., E. H. Lee, and S. J. Tupper, "The Theory of Wedge Indentation of Ductile Materials," Proc. Royal Soc. London, Series A, Vol. 188, 1947, pp. 273-291.
15. Tabor, D., The Hardness of Metals, Oxford: Clarendon Press, 1951.
16. Johnson, K. L., "The Correlation of Indentation Experiments," J. Mech. Phys. Solids, Vol. 18, 1970, pp. 115-126.
17. Lancaster, J. K., "Geometrical Effect on the Wear of Polymers and Carbons," Trans. ASME, Jl. Lub. Tech., Vol. 97, 1975, p. 187.

APPENDIX C

The Effect of Molecular Weight, Surface Roughness,
and Sliding Speed on the Wear of Rigid Polyvinyl Chloride

Norman S. Eiss, Jr., VPI&SU

Gary S. Vincent, Texas Instruments

Accepted for presentation at the American Society
of Lubrication Engineers at the Annual Meeting,
Pittsburgh, Pa., May 11-14, 1981
and for publication in ASLE Transactions

ASLE Preprint No. 81-AM-2D-1

ABSTRACT

The wear of rigid polyvinyl chloride PVC, was measured in a pin-on-disk apparatus as a function of PVC average number molecular weight (70000 and 40000), steel counterface roughness (0.15 to 1.27 $\mu\text{m } R_a$), and sliding speed (0.1 to 1.4 m/s). The lower molecular weight PVC had the higher wear at all test conditions except 1.4 m/s speed and 1.27 $\mu\text{m } R_a$. At this condition the calculated interface temperature exceeded the glass transition temperature of 74°C for PVC. The wear rate increased for increases in both surface roughness and sliding speed. These results were explained in terms of the increased penetration of the steel asperities into the PVC necessitated by changes in these two factors.

INTRODUCTION

The wear of polymers on hard, rough surfaces is dominated by the abrasive wear mechanism. Considerable progress has been made in the understanding of the interaction between the surface topography and the polymer properties in the abrasive wear process in single traversal sliding experiments (1-7)¹. These investigations provided the foundation for models of the polymer abrasive wear process which utilize the profile of the surface and polymer properties to predict wear to within a factor of 5 of the measured values (8, 9). In these referenced researches the sliding speeds were below 1 cm/s to avoid the complication of interfacial heating.

¹Numbers in parentheses are references listed at the end of the paper.

At sliding speeds above 1 cm/s in multiple traversal experiments several additional factors influence the polymer abrasive wear process. Interfacial heating and increases in strain rate cause the polymer properties to change from their room temperature, low strain rate values. Eiss and Bayraktaroglu (10) studied the influence of surface roughness and sliding speed on the wear of low density polyethylene (LDPE). This study showed that LDPE films formed on the smoothest surfaces tested while the abrasive wear mode dominated wear on the rougher surfaces. The temperatures at the interface were calculated to be less than that required for polymer melting.

The research reported in this paper was a continuation of the study of polymer wear in high speed, multiple traversal sliding. In this study, the wear of rigid polyvinyl chloride of number average molecular weights (MW_n) 70000 (PVC I) and 40000 (PVC II) was measured as a function of surface roughness of a steel counterface and sliding speed. In the experiments reported the sliding speeds were chosen so that the calculated interfacial temperature exceeded the glass transition temperature (T_g) of 74°C of the PVC. Thus, the wear mechanisms were studied as a function of the change in the mechanical properties which occurred as the interfacial temperature exceeded the glass transition temperature. In addition, the experiments were designed so that interactions between molecular weight, surface roughness, and sliding speed were detected.

EXPERIMENTAL

The experiments were performed on a pin-on-disk machine (11). Cylindrical pins, 1.58 mm diameter and 7.94 mm long, were machined from rectangular plates of rigid PVC I (70000 MW_n) and PVC II (40000 MW_n). The PVC had the following formulation: 2 per cent butyl tin stabilizer, 1 per cent acrylic processing aid, and 0.5 per cent lubricant. Compression molding conditions for all plates were: five minutes preheat, then five minutes pressure at 10.4 MPa with the platen temperatures at 190°C. Mechanical properties of the polymers, which were determined using an Instron tension tester and ASTM type IV tensile specimens (12) are listed in Table CI. T_g was found using differential scanning calorimetry to be 74°C for both PVC I and PVC II.

To afford intimate pin-disk contact during wear tests, a smooth flat was prepared on the end of each pin by rubbing on No. 220 sandpaper and then on NO. 00 emery paper. Pin ends were examined at 15X magnification. Loose particles were wiped off with a soft, dry cloth. Each pin was sealed in a marked plastic vial to minimize chances of contamination. Pins were handled at all times with tweezers.

Steel disks were machined from a bar of 1020 hot rolled steel to a diameter of 44 mm and thickness of 8.8 mm. The disks were ground with a unidirectional lay to three roughness, 0.15, 0.51, and 1.27 μm arithmetic average roughness, R_a. The disks were cleaned with running tap water to remove loose metal particles and for two minutes in methanol in an ultrasonic bath. After drying with a soft cloth they were stored in a desiccator.

Table C1
Polymer Mechanical Properties*

Property	PVC I	PVC II
Tensile Strength at Yield, MPa	60.4 (+ 0.3) [†]	60.9 (+ 0.4)
Tensile Strength at Break, MPa	52.8 (+ 1.4)	39.6 (+ 1.3)
Elongation to Break, m/m	0.66 (+ 0.08)	0.31 (+ 0.03)
Energy to Rupture, MPa(m/m)	30.1 (+ 1.9)	12.8 (+ 0.7)
Modulus of Elasticity, GPa	3.84 (+ 0.2)	3.88 (+ 0.2)

*Based on measurements from 10 tension test specimens (ASTM type IV) pulled to break at a constant strain rate of 5 mm/ min.

[†]Standard deviations are given in parentheses below the average measured values.

1

A stylus profilometer with an optical-flat reference datum was used to obtain surface profiles on the steel disks perpendicular to the lay of the grinding marks. The output signal of the stylus device was the input to an analog-to-digital converter and a data memory system, which digitized and stored the data sample. The sampling length of the surface was 1.56 mm, which was about one pin diameter. The surface parameters R_a , RMS (root-mean-square) roughness, skewness, kurtosis, maximum peak-to-valley height, and autocorrelation length were calculated from the digitized profile data using a high speed, digital computer and were used to describe the topography of the steel surface. Average values for these surface parameters are listed in Table C2 for the three roughnesses.

All experiments were run with a normal load of 4.9 N. The sliding speeds at the pin center were 0.10, 0.75, and 1.40 m/s. The high speed was the maximum possible with the wear apparatus and was attained by locating a pin at a radius of 19 mm on a disk, which was rotating at 700 rpm. Low and medium speeds were likewise attained at 7.5 mm, 130 rpm and 13 mm, 550 rpm, respectively. Since the pin diameter was 1.58 mm, the velocity variations at the inside and outside radii of the pin contact area were ± 10 per cent, 6 per cent and 4.2 per cent at 0.10, 0.75 and 1.40 m/s, respectively. The speeds were selected anticipating friction-generated temperatures at the polymer-metal interface to be above and below the glass transition of PVC. Tests were conducted in laboratory air at 25°C ($\pm 2^\circ\text{C}$ standard deviation over the testing period) and 62 per cent (± 4 per cent) relative humidity.

Table C2
Surface Parameters* for Steel Disks

Parameter	Smooth	Medium	Rough
R _a Roughness, μm	$1.50(10)^{-1}$	$5.08(10)^{-1}$	1.27
RMS Roughness, μm	$1.91(10)^{-1}$	$6.30(10)^{-1}$	1.62
Skewness	$-6.89(10)^{-1}$	$-2.37(10)^{-1}$	$9.70(10)^{-2}$
Kurtosis	3.87	2.95	3.33
Maximum Peak-to-Valley Height, μm	1.30	3.88	$1.00(10)^1$
Autocorrelation Length, μm	$2.04(10)^1$	$3.18(10)^1$	$3.71(10)^1$

*Based on four measurements from each of four disks of each roughness.

In summary, the experimental design consisted of two levels of PVC molecular weight, three roughnesses, and three sliding speeds; a total of 18 combinations.

Each experiment involved wearing a fixed pin on a spinning disk and recording the friction force for a chosen number of disk revolutions (passes). In order to study the wear process through the initial and steady states, the numbers of passes selected after preliminary tests were 400, 800, 1600, 2400 and 3200. Some sliding situations resulted in excessive pin wear, in which case, the lower numbers of passes were used. Before and after each wear test, the mass of the polymer pin used in the test was measured with an accuracy of ± 4 μg with a microbalance to determine the mass loss (pin wear) due to sliding on steel.

Disks with polymer deposits and worn pins were examined with the Scanning Electron Microscope. Each specimen was coated with a thin (20 nm) layer of gold-palladium alloy to furnish a conducting path to ground for electrons striking the specimen in the SEM. Representative photographs were taken of the wear evidence.

RESULTS

The measured wear of PVC I on steel is plotted as a function of number of passes and R_a roughness at a sliding speed of 0.10 m/s in Fig. C1. Wear rates were defined as the slopes of the wear curves (Fig. C1) mg/pass, divided by the sliding distance per disk revolution, m/pass, which were 0.047 m/pass at low speed, 0.082 m/pass at medium speed and 0.120 m/pass at high speed. A least squares linear regression was performed to obtain the slopes and projected y-intercepts for each wear curve. Mean values and 95 per cent confidence limits for the wear rates

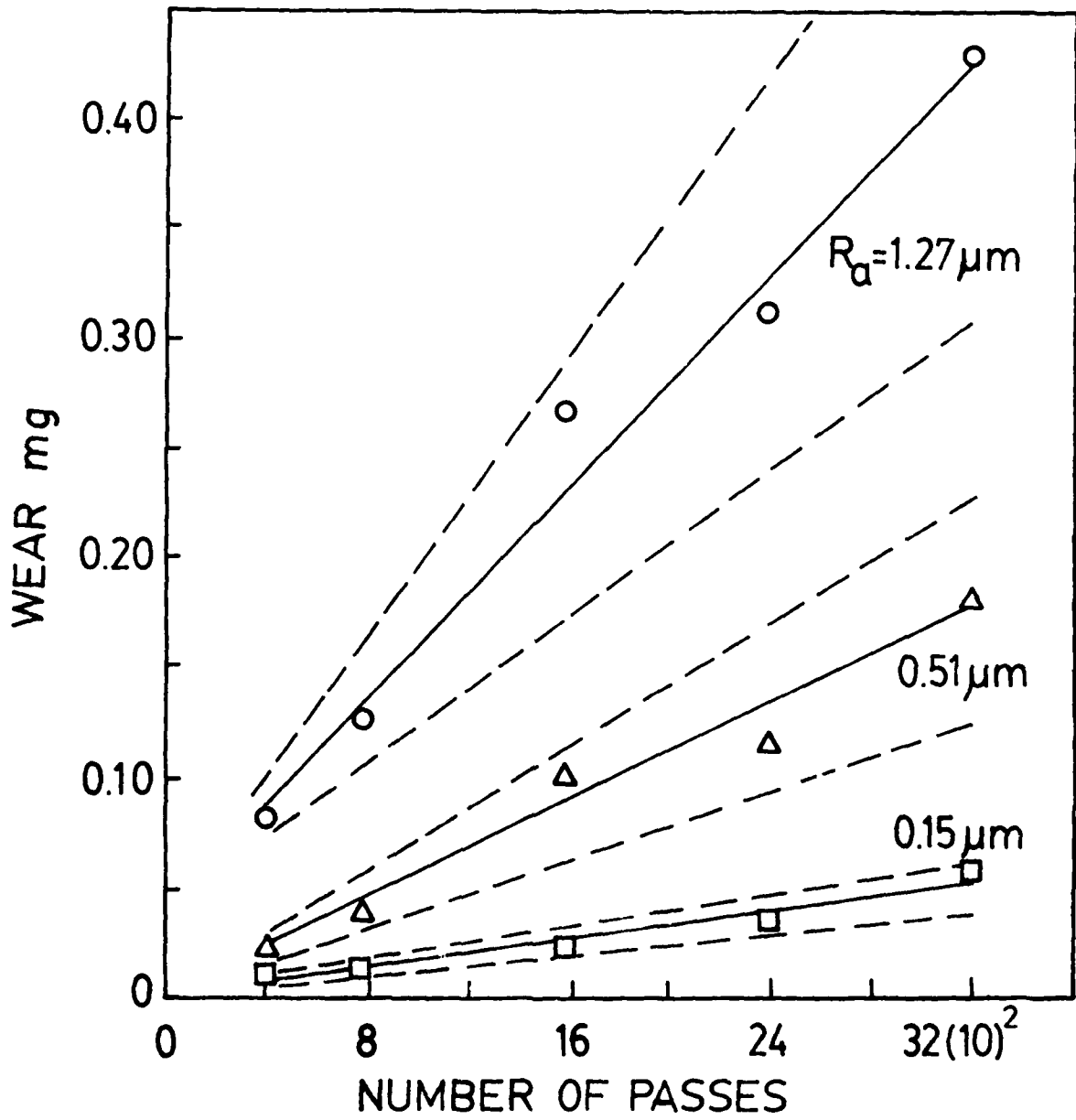


Figure C1. Wear of PVC I on steel as a function of number of passes and Ra roughness

are shown in Fig. C2. The only y-intercepts which were significantly greater than zero at the 95 per cent confidence level were for PVC I at 0.75 m/s on the roughest surface and PVC II at 0.75 and 1.4 m/s on the smoothest surface.

Friction coefficients are plotted for high molecular weight PVC on steel as a function of passes, sliding speed, and R_a roughness in Fig. C3. Large friction changes were noticed between 10 and 200 passes, after which essentially steady values were observed. In general, the effect of increasing sliding speed was to increase the friction coefficient. For example, on rough surfaces the coefficient of friction was 0.32 at low speed and 0.47 at high speed. For the low speed tests, sliding on smooth surfaces produced the highest friction, $f = 0.35$. The friction record for medium speed sliding on smooth surfaces coincided with that for high speed, so it was not shown in Fig. C3. No significant differences were noticed in the measured friction coefficients for the high and low molecular weight materials.

Friction-generated temperatures at the sliding interface were calculated using the model presented by Archard (13) modified for polymers sliding on steel (See Appendix 1). For the sliding velocities used in the experiments, 0.1, 0.75, and 1.4 m/s the values of the dimensionless speed parameter L were 0.4, 3.0, and 5.5, respectively. Using Eq. 1 in Appendix C1 for $L > 5$ the flash temperatures were calculated for 1.4 m/s. The flow pressure, p_m , was taken to be twice the tensile strength at yield (Table C1) based on data by Boenig (14). For mild steel, the

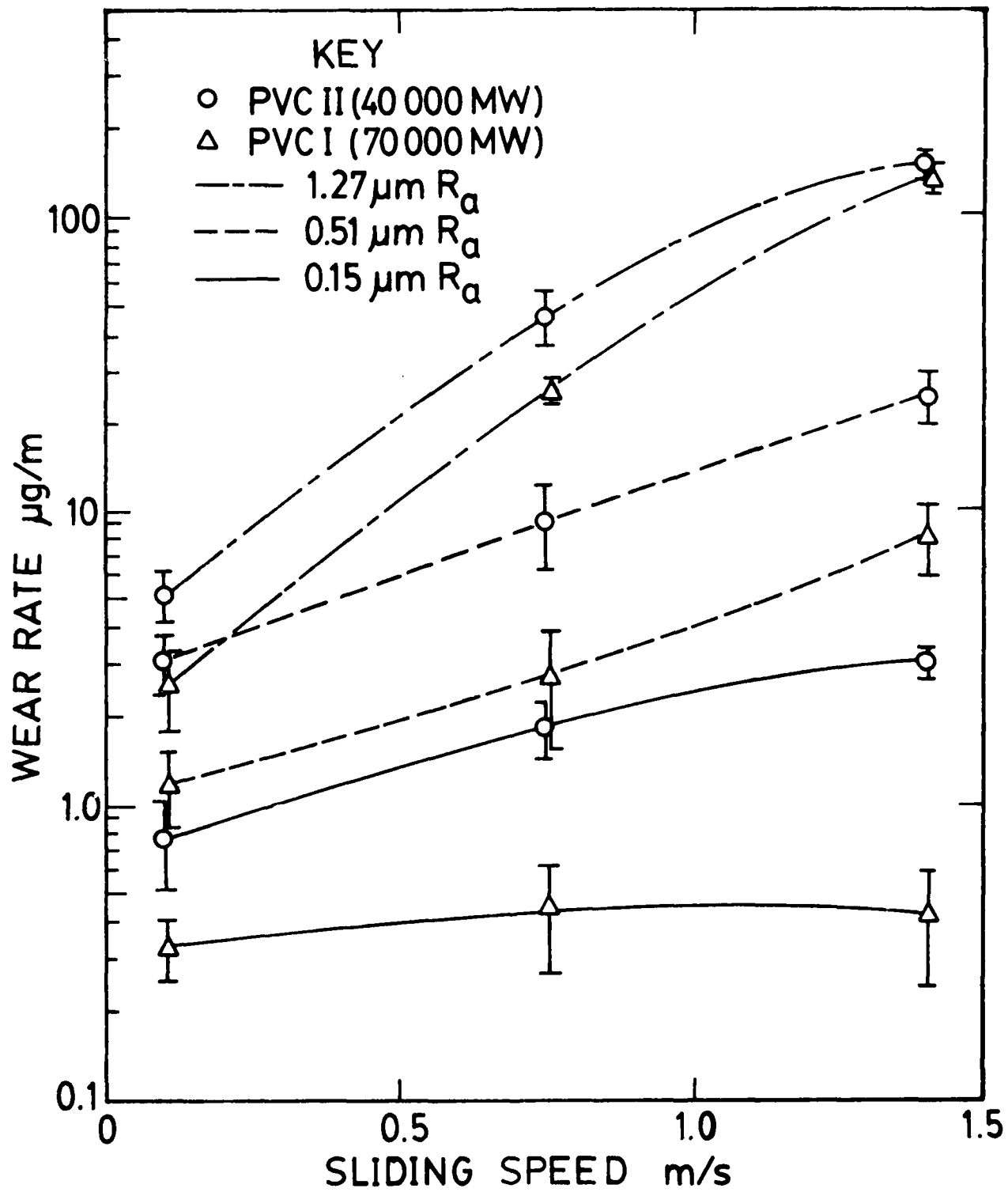


Figure C2. Wear Rate of PVC as a function of molecular weight, R_a roughness, and sliding speed.

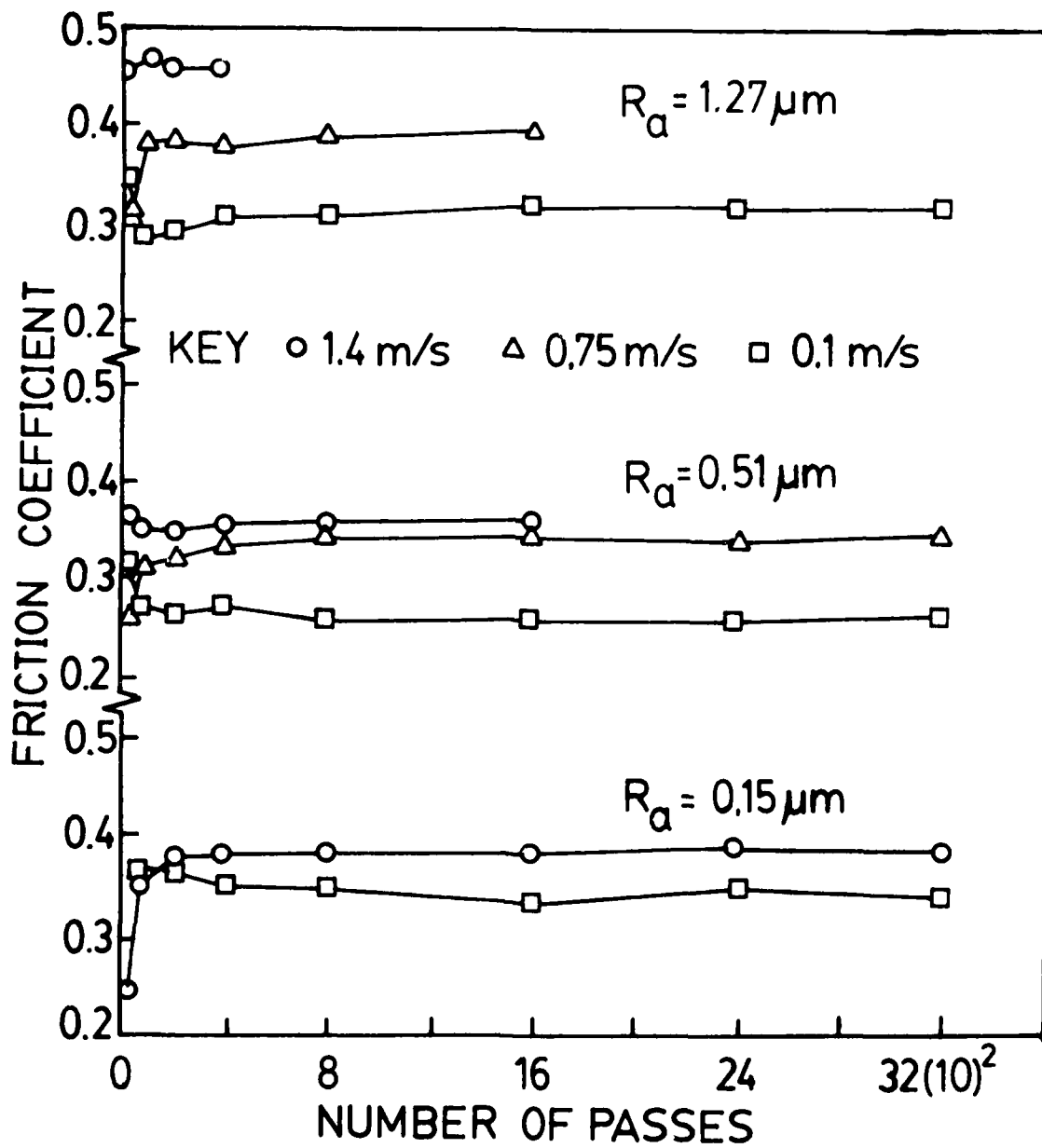


Figure C3. Coefficient of friction for PVC I sliding on steel as a function of number of passes, sliding speed, and R_a roughness

Table C3
 Calculated Surface Temperatures, PVC Sliding on
 Steel at 1.4 m/s

Polymer	R _a Roughness (μm)	μ	θ_m^* ($^{\circ}\text{C}$)	T _i [†] ($^{\circ}\text{C}$)
PVC I	0.15	0.38	45	70
	0.51	0.36	43	68
	1.27	0.48	57	82
PVC II	0.15	0.38	45	70
	0.51	0.38	45	70
	1.27	0.50	59	84

* θ_m = mean temperature rise at the interface

$$\dagger T_i = T_{\text{ambient}} + \theta_m = 25^{\circ}\text{C} + \theta_m$$

Note: T_g = 74 $^{\circ}\text{C}$

thermal conductivity and volume specific heat were taken as $47.0 \text{ W/m}^{\circ}\text{C}$ and $3.29 (10)^6 \text{ J/m}^3\text{ }^{\circ}\text{C}$, respectively (15). The calculated temperatures are given in Table C3.

DISCUSSION

The main effects of the molecular weight, roughness, and sliding speed on the wear rate of PVC are shown in Fig. C2. In general, the wear rate increased as the molecular weight decreased, the roughness increased, and the sliding speed increased. The interactions between these factors resulted in two deviations from these general main effects. At the highest values of speed and roughness, the difference in wear rates for the two molecular weights was insignificant. For the higher molecular weight (PVC I) and the smoothest surface, the wear rate was not significantly different for any speed. Some explanations for these observations are proposed in this discussion.

Molecular Weight

The inverse relation between molecular weight and wear rate observed for PVC has also been observed for polyethylene (PE) (16-18). In Ref. 17, PE pins with MW_n from 28000 to 70000 were run on polished steel disks at sliding speeds from 0.10 to 3.0 m/s. Over this speed range, the lowest molecular weight PE had a wear rate of approximately three times that of the highest molecular weight PE. As noted in Fig. C2 for the smoothest surface ($0.15 \mu\text{m } R_a$), the 40000 MW_n PVC II had an average wear rate of 4.6 times that of the 70000 MW_n PVC I. Thus, in spite of the many differences between PE and PVC (e.g., degree of crystallinity,

T_g , and mechanical properties), the influence of molecular weight on wear rate under similar test conditions is in the same direction and of the same order of magnitude for both.

Some insight on the relationship between molecular weight and wear can be obtained from wear experiments on PVC in which the molecular weight of the debris was compared to that of the slider (19). A PVC block was held against a mild steel ring polished to $0.075 \mu\text{m } R_a$. At a sliding speed of 1.4 m/s, the MW_n in the debris was 17,000 while that in the block was 31,000. In the discussion of this paper the author noted that when experiments were run above T_g , the MW_n of the debris was higher than that of the debris when run at temperatures below T_g .

The explanation offered was that wear was the result of both chain rupture and chain slippage. At temperatures below T_g , the chain slippage is hindered by the relative immobility of the chains and chain rupture becomes the predominant mechanism of debris formation. At temperatures above the T_g , the greater mobility of the chains permits them to slip by each other when subjected to stress rather than rupture the chain. Hence, the wear debris for experiments run above T_g have a higher MW_n than that for the debris generated at temperatures below T_g .

For wear experiments run below the T_g for PVC, PVC I with the higher molecular weight has a higher degree of chain entanglement and immobility than the lower molecular weight PVC II. Therefore, the PVC II has a higher probability of fracturing by chain slippage than PVC I. Since interchain forces are weaker than bonding forces within the chain, more fracture and more debris forms for the low molecular weight PVC II.

When the interfacial temperature exceed T_g such as at 1.4 m/s on the rough surface (see Table C3), then the chains achieve a high degree of mobility and chain slippage becomes the dominant mode of debris formation. Under this condition, the influence of the molecular weight on wear rate becomes insignificant as indicated in Fig. C2.

Surface Roughness

The increase in wear rate with roughness has been observed by several investigators (6, 10, 20). Lancaster's data (20) for the amorphous, more brittle polymers showed increases in wear rate of two orders of magnitude for an order of magnitude change in R_a roughness. The semi-crystalline, more ductile polymers typically had increases in wear rate of one order of magnitude for a similar change in R_a roughness.

The data for PVC have been replotted in Fig. C4 to emphasize the relationship between wear rate and roughness. The increases in wear rate vary from one to two orders of magnitude for an order of magnitude change in roughness, with the larger changes occurring at the higher sliding velocities. These and Lancaster's data emphasize that it is not possible to predict polymer wear based on the R_a roughness only.

However, the general trend of increasing wear with increasing roughness can be related to the number of asperities in contact with the slider and their average depth of penetration. These two parameters were calculated from the surface profiles as follows. At any reference ordinate height, the number of ordinate heights greater than the reference height divided by the total number of data points in the profile defines the bearing area ratio (BAR) for that height. The number of

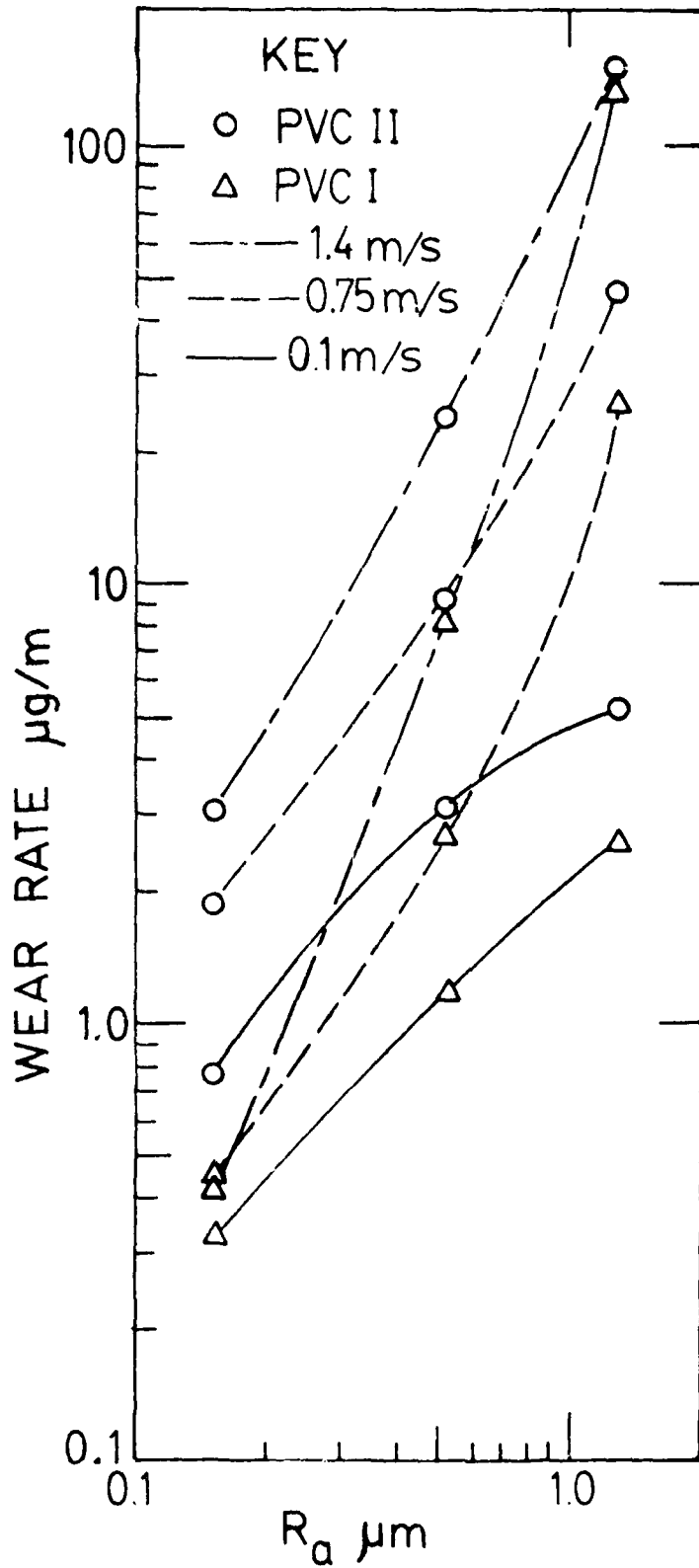


Figure C4. Wear rate plotted on log-log scales to show R_a roughness dependence

AD-A098 478

VIRGINIA POLYTECHNIC INST AND STATE UNIV BLACKSBURG --ETC F/G 11/9
THE WEAR OF POLYMERS BY TRANSFER TO HARD, ROUGH SURFACES. (U)
FEB 81 N S EISS

DAA629-77-6-0102

UNCLASSIFIED

ARO-14658.7-E

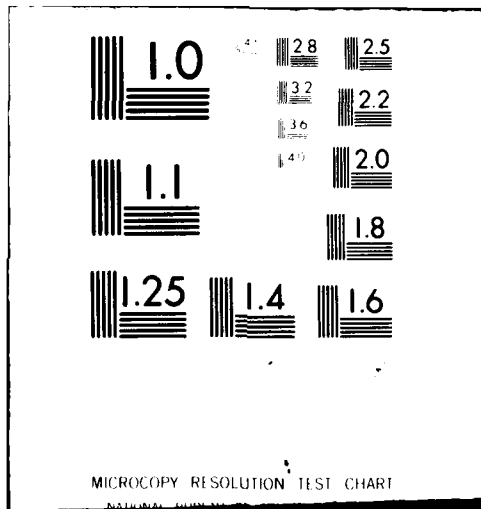
NL

2 of 2

200 200



END
DATE
FILMED
6-81
DTIC



MICROCOPY RESOLUTION TEST CHART
NATIONAL BUREAU OF STANDARDS-1963-A

peaks above the reference height were counted and the difference between the peak height and the reference height was the penetration depth for the peak. The number of peaks and the average penetration depth are tabulated in Table C4 as a function of BAR for the three different surface roughnesses.

In these experiments the ratio of the real area of contact A_r to the apparent area of contact A_a was calculated using $A_r/A_a = (W/p_m) / (\pi d^2/4)$ where W = normal load (4.9 N)

p_m = flow pressure (2 x yield strength = 2 x 60 MPa)

d = diameter of the PVC pin (1.58 (10)⁻³m)

Therefore $A_r/A_a = 0.0208$. This ratio is also the BAR; thus, the data in Table C4 for BAR = 0.02 apply to the results of the experiments run at 0.1 m/s where the yield strength is approximately equal to its room temperature value.

The data at BAR = 0.02 showed that the average penetration depth increased and the number of contacting asperities decreased as the surface roughness increased. However, the average penetration depth was over an order of magnitude larger for the rough surface than for the smooth surface while the number of contacting asperities on the rough surface was only a third of those on the smooth. Hence, the fewer contacting asperities on the rough surface must penetrate much deeper in order to develop sufficient real area to support the load.

As sliding occurs the polymer must either deform and flow around the asperities or fracture and form a wear particle. As the penetration depth increases, the amount of strain experienced by the polymer as it deforms in moving past the asperity must increase. Thus, as the likelihood of fracture rather than flow increases with the penetration

Table C4

Number of contacting Peaks and Average Penetration Depth

<u>BAR</u>	<u>Average Penetration Depth (μm)</u>			<u>Number of Peaks in 1.56mm</u>		
	<u>Smooth</u>	<u>Medium</u>	<u>Rough</u>	<u>Smooth</u>	<u>Medium</u>	<u>Rough</u>
0.02	0.04	0.17	0.66	15	10	5
0.04	0.05	0.20	0.79	25	16	10
0.06	0.06	0.22	0.80	35	24	14
0.08	0.06	0.24	0.85	42	29	17
0.10	0.07	0.25	0.87	51	35	21

depth, the wear per asperity increases. Therefore, in spite of decreased number of asperities in the rough surface, they generate more total wear than the larger number of asperities on the smooth surfaces.

The wear that occurs is also a function of the accumulation of the wear particles in the spaces between the contacting asperities. At one extreme, the accumulated debris could support a significant fraction of the normal load thus decreasing the fraction carried by the metal asperities. This shift in load from the asperities to the polymer debris would continue until the polymer pin was sliding predominantly on accumulated polymer debris and the wear mechanism would no longer be primarily abrasive. This shift in mechanism is more likely to occur on smooth surfaces because of the small volume of debris necessary to fill up the spaces. Some evidence for the different transfer to the surfaces of different roughness are shown in Fig. C5-8.

The topography of the smoothest surface was characterized by plateaus separated by grooves. Such a surface has negative skewness as shown in Table C2. The plateaus supported some of the normal load without causing significant abrasive transfer. As the polymer slid over the surface the oxide particles from the steel were picked up by the polymer and scratched the steel surface as shown in Fig. C5. Some polymer was abrasively removed at the edges of the plateau regions and at asperity ridges and these deposits gradually increased in size (Fig. C6) until they were picked up by the pin or dislodged and moved to the edge of the wear track. The SEM photos did not reveal any significant differences in the transfer of PVC I or PVC II to the smooth surfaces.

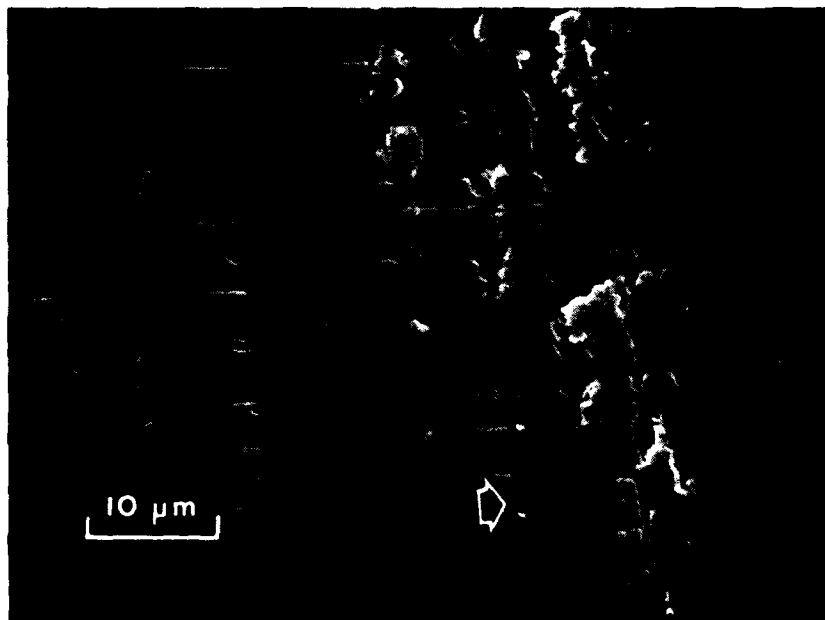


Figure C5. Steel surface with deposits of PVC I, 60 passes, 0.10 m/s

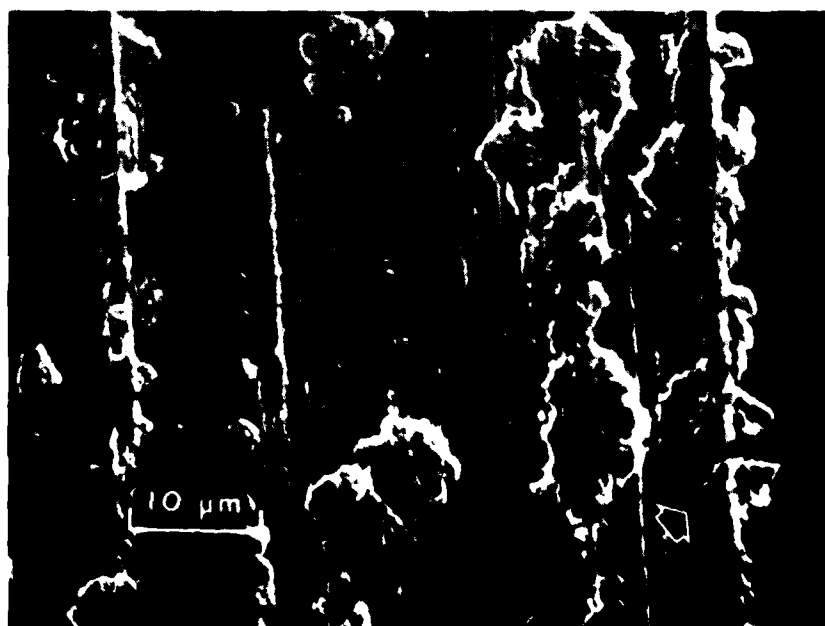


Figure C6. Steel surface with deposits of PVC I, 400 passes, 0.10 m/s

On the rougher surfaces, the height distribution was more Gaussian as evidenced by the smaller absolute values of skewness (a Gaussian surface has a skewness equal to zero). The PVC made contact with asperity peaks and transfer of particles occurred at the asperities (Fig. C7). The particles grew in size (Fig. C8) and eventually became detached and moved to the edge of the track.

Sliding Speed

The results in Fig. C2 showed that increases in sliding speed resulted in significant increases in wear rate except for PVC I on the smoothest surface. An increase in sliding speed causes both an increase in interfacial temperature and an increase in strain rate. A study of the effect of temperature and strain rate on the mechanical properties of PVC in a tensile test have shown that the temperature effect is dominant (21). For example, at a strain rate of 0.1 sec.^{-1} a change in temperature from 23 to 60 C reduced the yield strength from 48 to 24 MPa. At a temperature of 23 C, a change in strain rate from 0.1 to 1.0 sec.^{-1} increased the yield strength from 48 to 51 MPa. The data indicated that a change in strain rate of four orders of magnitude resulted in an increase from 48 to 69 MPa in the yield strength.

Elevated temperature tensile tests were performed on PVC I and PVC II. The data indicated that a change in temperature from 22 to 65 C reduced the yield strength from 60 to 6.9 MPa. At 70 C no yield point could be detected (Fig. C9, Appendix C2). The room temperature difference in elongation to break for PVC I and II disappeared at test temperature of 50 C and above.

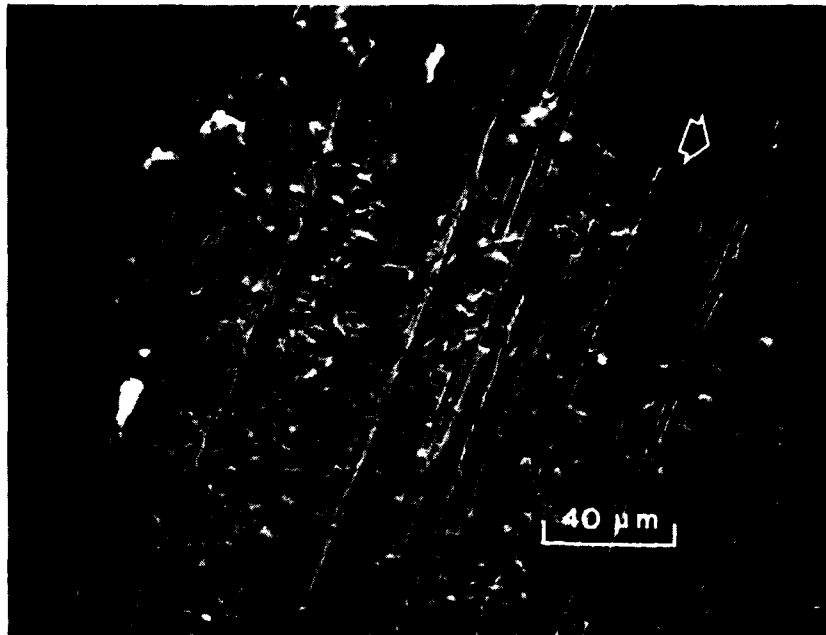


Figure C7. Steel surface with deposits of PVC II, 400 passes, 0.10 m/s

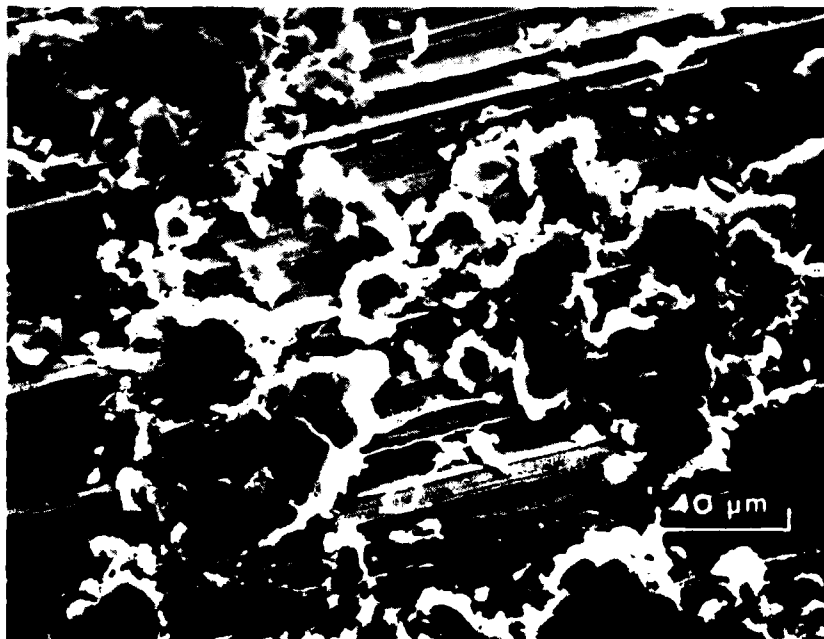


Figure C8. Steel surface with deposits of PVC II, 1600 passes, 0.10 m/s

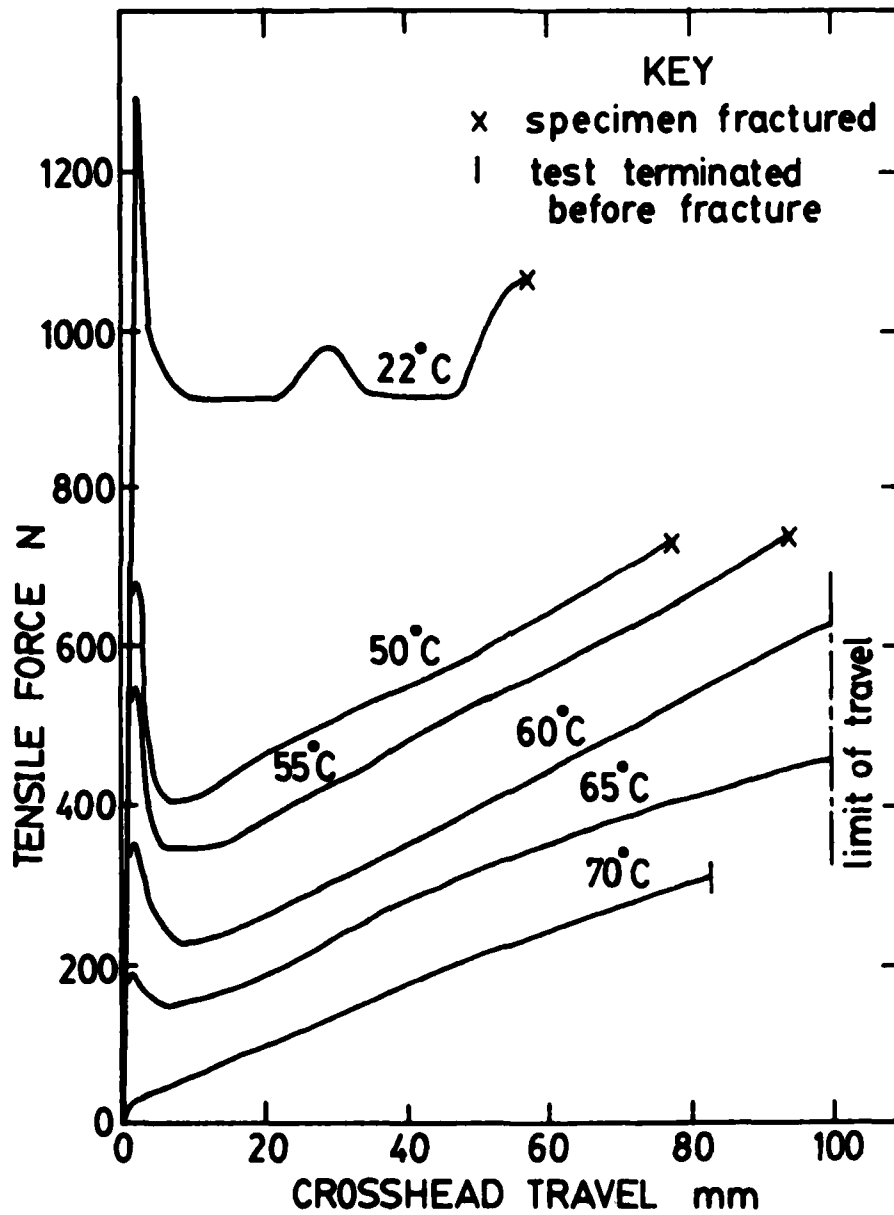


Figure C9. Tensile force versus cross head motion in elevated temperature tests of PVC I

J

The interfacial temperatures were estimated using Archard's equation (Appendix C1). At the sliding speed of 0.75 m/s the temperatures were approximately 60 C while the temperatures calculated at 1.4 m/s are given in Table C3. Thus, the result of the increase in sliding speed in the experiment was a reduction in the yield strength of the polymer. As noted in the discussion on roughness, the BAR was calculated using the polymer yield strength. As the yield strength decreased the BAR increased. Table C4 shows that the increase in BAR results in more asperity contacts and greater penetration per contact. Hence, the wear rate increases with increasing sliding speed.

Transient and Steady Wear

In sliding contacts, the wear rate is high initially and then decreases to some lower steady state value. In these experiments the first wear measurement was made at 400 passes. The comparison of the wear data at 400 passes with the linear regressions showed that the data were not significantly biased below the regression lines. If the transient state existed at 400 passes, then the wear at this distance would be less than predicted by the steady state regression line. Thus, it was concluded that steady state wear was established when the wear was measured at 400 passes.

If the transient wear occurs over a significant number of passes, its effect will be to cause the linear regression line of the steady-state wear to have a positive y-intercept. As noted in the results, only 3 of the 18 experiments had a significantly positive intercept. Thus, in 15 cases, the experimented scatter was great enough to obscure any evidence of the transient wear state.

CONCLUSIONS

1. The wear rate of PVC varied inversely with molecular weight when the interfacial temperature was less than T_g . When the interfacial temperature exceeded T_g , there was no significant effect of molecular weight on wear.

2. The polymer molecular weight affects wear primarily through the influence of chain length on molecular mobility at temperatures below T_g .

3. The wear rate of PVC varied directly as the surface roughness of the steel counterface. This dependence was caused by rougher surfaces needing greater asperity penetration depths to support the normal load.

4. The wear rate of PVC varied directly as the sliding speed. The changes in sliding speed caused changes in strain rate and interfacial temperature which resulted in changes in polymer yield strength at higher speed. The yield strength decreased which required more real area to support the normal load. The increased penetration necessary to increase the real area caused more wear to occur.

5. The wear measurements in these experiments were made during steady state conditions.

ACKNOWLEDGEMENTS

This work was supported by the U.S. Army Research Office, Research Triangle Park, N.C. and monitored by Dr. E. Saibel. The authors thank VPI&SU students Stephen McClesky for his helpful suggestions on interfacial temperature calculations and Brian Jacobeen who performed the elevated temperature tensile tests of PVC. The PVC was supplied by B. F. Goodrich Co., Chemical Division, Avon Lake, Ohio. The help of Messrs. Hugh Marty, G. Small, and Andrew J. Dito of B. F. Goodrich were greatly appreciated. The T_g for the PVC was measured on a Perkin-Elmer Differential Scanning Calorimeter, in the Characterization of Macromolecules Lab in the Chemistry Dept. of VPI&SU.

REFERENCES

1. Ratner, S. B., Farberova, I. I., Radyerkevich, O. V. and Lur'e, E. G., "Connection Between Wear-Resistance of Plastics and Other Mechanical Properties," in Abrasion of Rubber, Ed. James, D. S., MacLaren, London, 1967, p. 145.
2. Lancaster, J., "Abrasive Wear of Polymers," Wear, 14, 1969, p. 233.
3. Warren, J. H. and Eiss, N. S., Jr., "Depth of Penetration as a Predictor of the Wear of Polymers on Hard, Rough Surfaces," Trans. ASME, Jl. Lub. Tech., 100, January 1978, pp. 92-97.
4. Giltrow, J. P., "A Relation Between Abrasive Wear and the Cohesive Energy of Materials," Wear, 15, 1970, p. 71.
5. Lontz, J. F. and Kumnick, M. C., "Wear Studies of Moldings of Polytetrafluoroethylene Resin, Considerations of Crystallinity and Graphite Content," ASLE Trans., 16, 1973, p. 276.
6. Eiss, N. S., Jr., and Warren, J. H., "The Effect of Surface Finish on the Friction and Wear of PCTFE Plastic on Mild Steel," Soc. Manufacturing Eng., Paper No. IQ75-125.
7. Hollander, A. E. and Lancaster, J. K., "An Application of Topographical Analysis to the Wear of Polymers," Wear, 25, 1973, p. 155.
8. Eiss, N. S., Jr., Wood, K. C., Smyth, K. A. and Herold, J. H., "Model for the Transfer of Polymers on Hard, Rough Surfaces," Trans., ASME, Jl. Lub. Tech., 101, April 1979, pp. 212-218.
9. Herold, J. H., "A Model for Abrasive Polymer Wear," Ph.D. Dissertation, Virginia Polytechnic Institute and State University, Blacksburg, Va., June 1980.
10. Eiss, N. S., Jr., and Bayraktaroglu, M. M., "The Effect of Surface Roughness on the Wear of Low-Density Polyethylene," ASLE Trans., 23, 3, July 1979, pp. 269-278.
11. Eiss, N. S., Jr., Warren, J. H. and Doolittle, S. D., "An Application of Neutron Activation Analysis to the Measurement of Wear of Polymers." Wear, 38, 1976, pp. 125-139.
12. Annual Book of ASTM Standards, Part 27, American Society for Testing and Materials, Philadelphia, Pa., 1973, pp. 183-195.
13. Archard, J. F., "The Temperature of Rubbing Surfaces," Wear, 2, 1958, pp. 438-455.
14. Boenig, H. V., Structure and Properties of Polymers, John Wiley, New York, 1973.

15. CRC Handbook of Tables for Applied Engineering Science, Ed. Bolz, R. E. and Tuve, G. L., CRC Press, Boca Raton, Florida, 1976.
16. Pratt, G. C., "Plastic Based Bearings," in Lubrication and Lubricants, Ed Braithwaite, E. R., Elsevier Pub. Co., N.Y., 1967, pp. 403, 4.
17. Tanaka, K. and Uchiyama, Y., "Friction, Wear and Surface Melting of Crystalline Polymers," Advances in Polymer Friction and Wear, Ed. Lee, L. H., Plenum Press, N.Y., 1974, pp. 499-532.
18. Deanin, R. D. and Patel, L. B., "Structure, Properties, and Wear Resistance of Polyethylene," ibid, pp. 569-581.
19. Richardson, M. O. W., and M. W. Pascoe, "Mechano-Chemistry and Polyvinyl Chloride Wear," ibid, pp. 585-597.
20. Lancaster, J. K., "Relationships Between and Wear of Polymers and their Mechanical Properties," Proc. Instr. Mech. Eng., 183, 3P, 1968-1969, pp. 98-106.
21. Gomex, I. L., "Testing Rigid PVC Products--Analysis of Test Results," in Encyclopedia of PVC, 3, Ed. Nass, L. I., Marcel Dekker, Inc., N.Y., 1977, pp. 1593-1694.

APPENDIX C1 Flash Temperature Equations

According to Archard (13) the maximum attainable flash temperature occurs when the applied load is borne by plastic deformation at a single circular area. The value of the dimensionless parameter L determines which equation should be used to calculate the flash temperature, θ_m .

For $L > 5$

$$\theta_m = 0.435 \gamma NL^{\frac{1}{2}} \quad \dots 1$$

$$\text{where } N = \frac{\mu g \pi p_m}{J \rho c} \quad \dots 2$$

$$L = \frac{W^{\frac{1}{2}} V}{2\alpha (\pi p_m)^{\frac{1}{2}}} \quad \dots 3$$

$$\gamma = 1/[1 + 0.87 L^{-\frac{1}{2}} (K_1/K_2)] \quad \dots 4$$

μ = coefficient of friction

g = acceleration due to gravity

p_m = flow pressure

ρ = density

c = specific heat

W = normal load

V = velocity of the heat source or speed of sliding

α = $K/\rho c$ thermal diffusivity

K_1 = thermal conductivity of the body with a stationary "hot spot"

K_2 = thermal conductivity of the body with a moving "hot spot"

Archard assumed that $K_1 = K_2$ in his derivation of Eq. 4. For $K_1 = K_2$, Eq. 4 can be derived following the steps in Archard's paper. For polymers sliding on steel, K_1/K_2 is approximately equal to 0.005. Thus, for $L = 5$, $\gamma = 0.998$. Therefore, Eq. 1 can be used to calculate flash temperatures for polymers sliding on steel for $L > 5$ with sufficient accuracy by setting $\gamma = 1.0$.

APPENDIX C2 Elevated Temperature Tensile Tests

Elevated temperature tensile tests on PVC I and II were performed using a crosshead speed of 5 mm/min. Tests were run at 22.2°C, and 50 to 70°C in five degree increments. The temperature was allowed to come to equilibrium before each specimen was pulled. Fig. C9 is a composite of the charts from the testing machine showing the force versus the crosshead motion for PVC I. PVC II showed similar trends but with less elongation at 22°C as indicated on Table C1. At the higher temperatures there was no significant difference in the elongations between PVC I and II.